Surface Runoff on Green Urban Areas

A study on driving forces behind surface runoff generation

Erik Nilsson

Civilingenjörsprogrammet i miljö- och vattenteknik

Erik Nilsson

Abstract

Recent flooding events, such as the one in Germany 2021 have caused irreversible damages to infrastructure and lives. The aftermath of events like these have underlined the importance of an accurate risk management by predicting them in urban areas. This is done by hydrological modelling in which topography and presence of hardened surface often determine the magnitude of the flood. However, the contributory part from green areas to a flooding event is often simplified by a runoff coefficient not taking all of the soil hydraulic properties into account.

This thesis aims to study the surface runoff generation from three different soil types from different green urban areas in Uppsala, Sweden. Simulations have been conducted using the modelling tool Hydrus 1-D and two different types of rainfall-runoff simulations were investigated. Firstly, a 25-year historic rain series was simulated to investigate what soil moisture content was present in the soils before large rain events and what the main driving force for surface runoff generation was. The second part of the simulations was conducted using five type hyetographs depicting large rain events in Sweden. The aim of these simulations was to further investigate main driving forces for surface runoff generation and to examine if the temporal distribution of a rain event effect the surface runoff generation.

The results showed that the soil moisture content present in the soils before large rain events were very close to the field water holding capacity and that the main driving force for surface runoff generation on the studied sites was peak precipitation intensity, but also that the mean precipitation intensity and soil moisture had a significant effect within a 95 % confidence interval. The hyetograph simulations showed that the temporal distribution of a rain event effects the surface runoff generation on the studied soil, with the events whose peak came later generally generated more surface runoff.

Keywords: surface runoff, urban green area, soil moisture

Referat

Ytavrinning från gröna urbana områden

Erik Nilsson

Naturkatastrofer som översvämningar har på senare tid blivit mer omtalade och har orsakat enorma skador och kostnader på samhällen runt om i världen. Efterdyningarna av översvämningar likt den i Tyskland 2021 har betonat vikten av att på ett effektivt sätt hantera och försöka förutspå liknande händelser för att förebygga och därmed minimera skadorna. Detta arbete börjar ofta med en skyfallskarting där särskilt utsatta områden kan punktmarkeras. Flera av modellerna som utför skyfallskarteringar i urbana områden lägger stor vikt på topografi och utbredningen av hårdgjorda ytor för att uppskatta skaderisken av olika regn. Den delen av vattnet som har sitt ursprung från gröna ytor räknas ofta fram genom att ansätta en avrinningskoefficient som anger hur mycket av regnet som faller på ytan som rinner av. Detta tillvägagångsätt tar inte hänsyn till hur jordens olika hydrauliska parametrar kan påverka avrinningen och hur olika initiala markmättnader kan påverka ytavrinningen.

Detta arbete syftar till att undersöka ytavrinningen från gröna områden i städer med hjälp av empiriska värden hämtade från tre olika grönområden i Uppsala, Sverige. Två typer av simuleringar kommer utföras med hjälp av modellverktyget Hydrus 1D. Den första innehåller en 25-årig regnserie hämtad från regnstation i Stockholm och syftar att undersöka vilken markmättnad jordarna hade innan regnevent och vilken parameter som har störst påverkan på ytavrinningen. Den andra delen av simuleringarna gjordes med fem typhyetografer som ska efterlikna kraftiga regnevent i Sverige och syftar att vidare undersöka viktiga parametrar för ytavrinningsbildning samt hur den temporala variationen av ett regn kan påverka ytavrinningen.

Resultaten från den historiska regnserien visade att markmättnaden i jordarna innan regnevent var väldigt nära fältkapaciteten och den huvudsakliga parametern som påverkade ytavrinningen var den maximala 15 minuters regnintensiteten, andra parametrar som påverkade ytavrinningen signifikant under ett 95 % konfidensintervall var medelintensiteten och initiala markmättnaden. Resultaten från hyetografsimuleringarna visad att den temporala variationen av ett regn påverkar ytavrinningen, där regnevent vars maxintensitet skedde senare under eventet generellt genererade mer avrinning.

Preface

This study concludes the course "Degree Project in Environmental and Water Engineering" within the Master's Programme in Environmental and Water Engineering at Uppsala university. The study has been conducted in collaboration with supervisor Johan Kjellin at Tyréns and subject reader Benjamin Fischer at Uppsala university. I would like to thank them both for the support and guidance throughout this project. I would also like to thank Sara Ekeroth at Tyréns for supporting me with the field experiment, Daniel Erdal for helping me out with the modeling part, and all my colleagues at the Tyréns office in Uppsala for keeping me company during the making of this thesis.

I would also like to thank all my friends and family for keeping my mind in the right place and continue to focus on what makes me happy. Finally, to my closest friends here in Uppsala, Ciggpausgruppen – A big thank you for the continuous support throughout my studies and for all the fun memories.

Erik Nilsson

Uppsala

2023-02-21

Populärvetenskaplig Sammanfattning

Naturens krafter är något som alltid har påverkat vårt sätt att leva och var vi väljer att bosätta oss. Tillbaka i tiden under jordbrukssamhället levde folk mer utspritt men i takt med den industriella revolutionen valde fler att flytta ihop för att ta del av de möjligheterna som erbjöds av företagen. Urbaniseringen innebar att områden som tidigare stått orörda omvandlades till bebyggelse, vägar och andra anläggningar som var nödvändiga för att husera det stora antal människor som sökte sig till arbete i städerna. Urbaniseringstrenden fortsätter och naturens krafter utmanar allt mer. De negativa konsekvenserna tar sig i uttryck i form av till exempel översvämningar i våra städer. Problem med översvämningar får konsekvenser för både individ och samhälle. Det finns ett behov av beredskap och att anpassa befintliga lösningar till de förändrade förutsättningar som urbaniseringen och klimatförändringar innebär.

På senare tid har frågan kring klimatförändringar blivit mer uppmärksammad och när IPCC släppte sin rapport för 2021 indikerade den för kraftigare och mer frekvent extremväder. Skyfall förväntas ske oftare och regnintensiteten förväntas öka med cirka 7 % per grads uppvärmning av medeltemperaturen. Hur förbereder då städer sig för kraftigare skyfall?

I Sverige görs undersökningar där kraftiga regn simuleras digitalt över en konstgjord yta som ska återspegla verkligen och särskilt utsatta områden kan identifieras, en så kallad skyfallskartering. Dagens skyfallskarteringar simulerar översvämningens utbredning i rummet och i städer ansätts stora delar av ytan som hårdgjord, där den största delen av regnet som faller på ytan ej infiltrerar. Det som inte tas i hänsyn i någon högre grad är förmågan att infiltrera vatten hos gröngjorda ytor som exempelvis parker. I Sverige utgör parker en betydande del av stadsarealen och hänsyn bör därför tas till dessa ytor i en skyfallskartering.

Denna studie syftar till att undersöka hur mycket avrinning de gröna ytorna generat historiskt och vad som har störst påverkan på avrinningsbildningen. Detta gjordes genom att simulera nederbörd som fallit över Stockholm de senaste 25 åren över en modell som tar stor hänsyn till markens egenskaper. Fem regnevent som ska representera olika kraftiga svenska regn simulerades för att undersöka hur variation av regnintensitet under ett event kan påverka avrinningsbildningen.

Resultaten i denna studie visade att den parameter som främst påverkade avrinningsbildning på de undersökta svenska grönytorna var maxintensiteten under regneventet. Andra parametrar som hade en betydande påverkan på avrinningsbildningen var markmättnaden, det vill säga vattenhalt i marken, och medelintensiteten. Gällande de fem kraftiga svenska regnen visade det sig att de regn som hade högst maxintensitet, mer specifikt mot slutet av simulationen generellt sett gav större mängder avrinning. Detta förklarades med att markmättnaden uppnått högre värden innan maxintensiteten inträffade.

1. INTRODUCTION

As the world grows more populous and technologically advanced, more people seek to live in the cities, a phenomenon called urbanisation. To house the increasing population old buildings are repurposed to house more inhabitants and green areas are turned into housing blocks. With this changing land-use, permeable grass fields and forests are turned into hard-made surfaces of asphalt and concrete. This leads to an overall decrease in permeable areas which causes more of the stormwater to runoff the surface instead of infiltrating into the soil. The stormwater is then transported over the hard-made surfaces either into a storm drain or along the streets to the topographically lowest point, which in many cases floods (European Union, 2013).

In Sweden most of the stormwater management systems are designed for rain events with a return time of 5-10 years. This means that the system is designed to handle the largest rain event that is expected to occur in a 10-year span. The system will not be able to handle a rain event that exceeds these boundaries which means that the city is dependent on systems that can take care of the excess stormwater. Another problem in Sweden is that many older properties have a combined stormwater system which means that a singular system is used to transport both stormwater and sewage. This increases the risk of the system flooding during harsh rain events (Svenskt Vatten, 2007).

To avoid urban flooding, modern cities have plenty of available options that could be applied to dampen the effects. Retarding basins, permeable asphalt and more effective drainage systems are all good options to decrease the risk of flooding. However, the actual effect of these solutions vary depending on where they are placed in the city and for what magnitude of precipitation they are designed for (Starzec et al., 2020). One of the most effective ways to handle stormwater runoff as well as contributing to sustainable development are urban parks, as green areas generally are seen as good infiltration surfaces.

Green urban areas in Sweden are very abundant and account for a large part of city landscape. They are an important part of the urban environment and help contribute to overall well-being, cleaner air as well as creating urban ecosystems. Green urban areas are also good at retaining water due to the higher infiltration capacity in soils compared to hard-made surfaces (SCB, 2015). The amount of precipitation able to infiltrate during a short intensive rain is about eight times higher in a park than on an asphalted surface (Svenskt Vatten AB, 2016). This, the health benefits, and the overlying 11th goal for sustainable development "To make cities inclusive, safe, resilient and sustainable" are all contributors to why green urban areas account for 63% of the land use in Swedish cities. Many of the green urban areas close to the city centre are man-made and the upper layers of soil have been switched out with more nutrient rich soil to create optimal growing conditions for plant life. (SCB, 2015).

In recent times, like the flooding in Stockholm in May 2021, it has been noticed that rain events with relatively short return times (1-5 years) can result in floods more commonly related to heavy rainfall with return times over 100 years. The reason for these severe floods

could partly be due to high antecedent moisture limiting infiltration rates and therefore causing unexpected high runoff generation.

The relation between soil moisture and runoff generation has been captured with both field experiments and model simulations. A study done by Nielsen (2019) investigated runoff characteristics of an urban pervious catchment in Lystrup, Denmark during the fall-winter season. Nielsen used a rainfall simulator sprinkler system to produce a wide range of rainfall intensities and collected and measured the generated runoff. Nielsen found that the most dominant runoff generating process was subsurface throughflow, followed by saturation excess runoff. The study did not record any infiltration excess runoff during the time frame of the study. Regarding the most important soil parameter effecting runoff, Nielsen observed the highest correlation with soil water content, and only observed saturation excess runoff and subsurface throughflow if the soil volumetric water content was above 0.43 m^3 H_2O/m^3 soil (Nielsen, 2019). Nielsen's study gives an outlook on the dominant runoff processes in a green urban area in the northern temperate zone. However, field experiments like this often come with logistical limitations. In this case, the sprinkler system was not able to simulate rain intensities above 2.75 mm/minute, making it unable to simulate the most intense parts of some historic cloudbursts. Also, since the study was conducted during the fall-winter season the initial soil moisture was higher than what would be expected during the typical cloudburst season in Sweden (May-September). The field experiment was conducted on a plot scale, only measuring the runoff from a certain area with soil properties limited to that specific site. To achieve more general data representing runoff processes present on a larger scale, several different sites have to be investigated, and the requirements for upscaling Nielsen's experiment are very steep. A different approach would be to use hydrological models to simulate the experiment on a synthetic soil.

Hydrological modelling can be used to avoid field limitations but the hydrological processes in these models are often simplified, and it is unclear on how well they represent reality. The hydrological models commonly used today are physically based or conceptual models. The conceptual hydrological models are based on conceptual storages and parameters that need to be calibrated before usage, or they mimic simplified physical processes such as moisture accounting without considering energy fluxes. Physically based hydrological models rely on known scientific principles of the fluxes of energy and water in a system. Hydrological processes related to the land phase are often considered for the physically based models. These components include processes such as: evapotranspiration, surface runoff, snowmelt, interception, subsurface runoff, and channel routing. These processes occur naturally and are assumed to be valid for all events, including events that have not yet been observed, making physically based models a good choice when investigating extreme weather events.

To accurately represent the processes in a physically based model requirements for highly detailed data follow. This data could either be acquired from empirical measurements which represent the actual state at the studied site, with some limitations from the tools used. Detailed empirical data sets are rarely available and sometimes synthetic data must be used. Synthetic data is artificial data generated from an original data set with the purpose of reproducing the

sought after characteristic. Synthetic data is only as good as the original data set and suffer the same error sources as empirical data would but is a great tool when data is scarce. One issue with using synthetic data is that it does not include outliers seen in empirical data. Outlier could be seen as "errors" and removed from the data but it could also represent an important characteristic at the studied site (Reimann, n.d.).

Different hydrological models can also differ in how spatial variability is considered. Conceptual models are often classified as lumped models, which indicate that the spatial variability of a watershed characteristics is overlooked, and an average is set for the entire area, this representation is also called black box. The lumped model approach could be useful in situations where available data is scarce and research area large and is proven to give reasonable estimations. Physically based hydrologic models are either fully distributed, where a river basin could be discretized as a grid mesh, or semi-distributed, where the basin could be divided into several sub-basins based on its characteristics (Islam, 2011).

To identify dominant runoff processes for a catchment it is required to link them to the underlying hydraulic capabilities of a soil. Generally, two different approaches are used to create this link, bottom-up, and top-down. The bottom-up approach relies on detailed soil data and rainfall simulations to identify dominant runoff processes for a certain plot. These processes are then assigned to areas with similar properties to create a large network to represent a catchment. The top-down approach does not require as detailed data sets but instead identifies catchment areas with similar characteristics from course data sets like aerial photos and existing geological maps. These areas are then lumped as hydrological homogenous regions assumed to be governed by the same dominant runoff processes (Seiberg & Rinderer 2012).

Ravn et al. (2018) investigated the relation between antecedent conditions and runoff using Horton's equation, an equation that calculates the infiltration capacity using soil specific constants and precipitation duration. Historic rainfall records from Copenhagen, Denmark was simulated on four different soils and the runoff calculated. The issue with this type of modelling is that it does not consider the fate of the water after it had infiltrated into the soil and assumes that it disappears once entering the soil profile. The Horton equation is highly dependent on rain duration and does not reflect the impacts soil moisture have on infiltration rates (Ravn et al., 2018). Further research on the dynamics of soil water content and excess rainfall is needed to achieve a greater understanding of the different hydrological processes and driving forces behind surface runoff generation on green urban areas.

2. AIMS AND OBJECTIVES

The purpose of this thesis is to, with the help of the soil model Hydrus 1D, investigate the effect of antecedent soil moisture in the upper soil layers (0-40 cm), and what it has been at the start of historic heavy rain events in Uppsala, Sweden. This thesis also aims investigate the dynamics of soil water content and excess rainfall during rainfall events. This aims to help better understand the surface runoff contribution from urban green areas in Sweden and better predict the magnitude of urban floods.

The report aims to answer the following research questions:

- What impact does antecedent soil moisture have on the generation of surface runoff from a Swedish green urban area?
- What is the main driving force for surface runoff generation on a Swedish green urban area?
- What soil moisture content was present in the soil before historic cloudbursts?
- Does the temporal distribution of a rain event affect runoff generation?

3. THEORY

3.1 INFILTRATION MECHANISMS

Knutsson and Morfeldt (1973) defined infiltration as a fluid's permeation into a porous media or a cracked frame. Infiltration is followed by the movement of a fluid through a medium, a process called percolation (Knutsson & Morfeld, 1973). The amount of water able to infiltrate is determined by the infiltration capacity of the medium. Infiltration capacity was defined by Richards (1952) and the Soil Science Society of America (1956) as the maximum rate at which a soil will absorb water impounded on the surface at a shallow depth when adequate precautions are taken regarding border effects (Johnson, 1963). Three main factors are said to determine the infiltration capacity of a soil: the initial entry of water into the soil and vegetation, the movement through the unsaturated zone, and the storage capacity. The least of the three factors is assumed to determine the infiltration capacity.

The initial entry of water is determined by the presence of vegetation which can intercept water droplets from entering the soil surface, macropores created by roots can also greatly affect the initial entry. The soil type of the upmost layer also plays an important part, if a thin layer of silt or clay particles cover the surface, once water is added, these particles can create a "seal" on the surface decreasing the infiltration rate. Another limiting factor is the characteristics of the lower soil layers as water cannot enter the profile faster than it is transferred away.

The infiltration capacity of soil is considered the largest hinderance of rainwater in natural areas. Once it has been reached, most of the excess precipitation will become surface runoff. For most rain events in temperate climates on natural areas, the infiltration capacity is higher than the precipitation intensity and all the rainwater is allowed to infiltrate. In rare events, high intensity rainfall can cause the infiltration capacity in the upper layer to be surpassed and generate runoff, this may happen even though lower layers remain unsaturated (Johnson, 1963).

Generally, infiltration capacity is higher in sandy coarser soils than in clayey soils with distribution and grain size often determining the infiltration capacity. However, exceptions such as macropores in finer clay soils which leads to preferential flow paths or compacted coarser soils occur (*Certified Crop Advisor Study Resources (Northeast Region)*, n.d.).

3.2 BULK DENSITY

The bulk density is a measure of the mass of a known volume, and it is calculated by dividing weight of a sample with the bulk volume. It gives an indication of organic matter, porosity, and soil texture. Generally, bulk density increases with profile depth due to it being less porous and more compacted. A normal distribution of bulk densities for clay is 1.0 to 1.6 g/cm^3 and for sand is 1.2 to 1.8 g/cm^3 (Chaudhari et al., 2013).

3.3 HYDRAULIC CONDUCTIVITY

Hydraulic conductivity is the capacity of a porous media to transmit fluids. The hydraulic conductivity depends on soil properties, such as saturation and bulk density, and fluid properties, such as viscosity and specific weight. Due to heterogenic properties of a soil, the hydraulic conductivity often varies greatly throughout a soil profile (Oosterbaan & Nijland, 1986).

3.4 WATER RETENTION

Different soil types have different capacities to retain water in the profile. Fine textured soils such as clays generally have the largest pore space, and more water can be stored in the profile than in other soils. A clay soil often consists of a multitude of small pores, micropores, and course textured soils generally have large pores. The pore size distribution determines the water retention of the soil, a clay soil with small pores generally has a greater surface area than a soil with large pores, which generates a stronger adhesive force counteracting the draining gravitational force. The large pores in course textured soils exert fewer adhesive forces causing water to more easily drain in the profile (Yasuda, 2023).

Soil water content is often described using three different levels, wilting point, field capacity, and saturation. The permanent wilting point is the point when there is no available water for plant uptake, this point is different for different crops but generally occurs around a suction of 1500 kPa. At the wilting point there is still some water in the soil, but the plants require a suction force of 1500 kPa to extract the water. The soil moisture at wilting point depends on the soil type, but generally courser textured soils retain less water (~10%) than finer textured soils (~28%).

The field water holding capacity is the amount of water that a soil can retain after being saturated and allowed to drain for 1-2 days. This is approximately equal to a tension of -0,33 bar being exerted on the soil water. The field capacity is considered to be ideal for crop growth.

Saturation is the state when all soil pores are filled with water and there is no air left in the soil. This state rarely last for longer periods as the soil water will drain to lower levels, starting with the largest pores. This drainage process occurs faster in course textured soils (3-6 hours) than in finer textured soils (2-3 days) (Rai et al., 2017).

3.5 CLOUDBURSTS

A cloudburst is an extreme weather event that often causes catastrophic damages and costs for the society. They are often characterized as sudden, very heavy, local brief rain events. In Sweden, a cloudburst has happened at least once per year since 1990. Cloudbursts are often

very local and are therefore hard to accurately measure with common rain gauges. Sveriges Meteorologiska och Hydrologiska Institut (SMHI) has defined a cloudburst as a rain event in which at least 50 mm rain falls during an hour or as a rain event with the intensity of 1 mm/minute (Olsson et al., 2017).

3.6 RUNOFF GENERATING MECHANISMS

There are three main runoff generating mechanisms that contribute to flooding. These three are Horton overland flow, subsurface flow, and saturation excess flow.

Horton overland flow or infiltration excess overland flow is a runoff mechanism that is created due to surface water input exceeding the infiltration capacity of a soil. This causes the excess water to accumulate on the soil surface and run off along the surface topography. Horton overland flow is commonly seen in irrigated fields and in urban areas, mainly on hard-made surfaces, and more generally during heavy rainfall events. Its occurrence is also commonly seen on soils with low infiltration capacities, such as clay, as well as compacted soils (Buda, 2013).
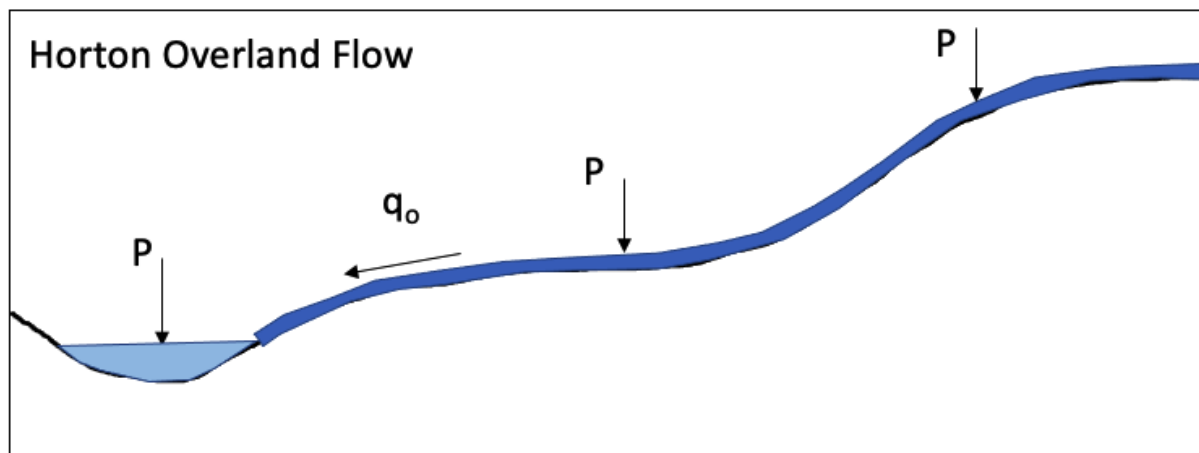
FIGURE 1: DEPICTING HORTON OVERLAND FLOW, ARROWS INDICATING PRECIPITATION (P) AND OVERLAND FLOW (Q_o), (FOLLOWING BEVEN, 2000)

Subsurface flow accounts for the flow that occurs underneath the soil surface and mainly consists of groundwater. It can be defined as the water that penetrates the soil and becomes the main runoff generating mechanism when the soil's infiltration rate exceed the rainfall intensity (Kiani-Harchegani et al., 2022). It is mostly seen in humid environments and steep topography with conductive soils that allows horizontal flow in the soil profile. Furthermore, subsurface flow generally occurs where the hydraulic conductivity decreases with depth. Subsurface flow can also occur in drier climates with gentler topography, however, only during extreme conditions such as high intensive rainfall and high antecedent soil moisture (Weiler et al., 2006).
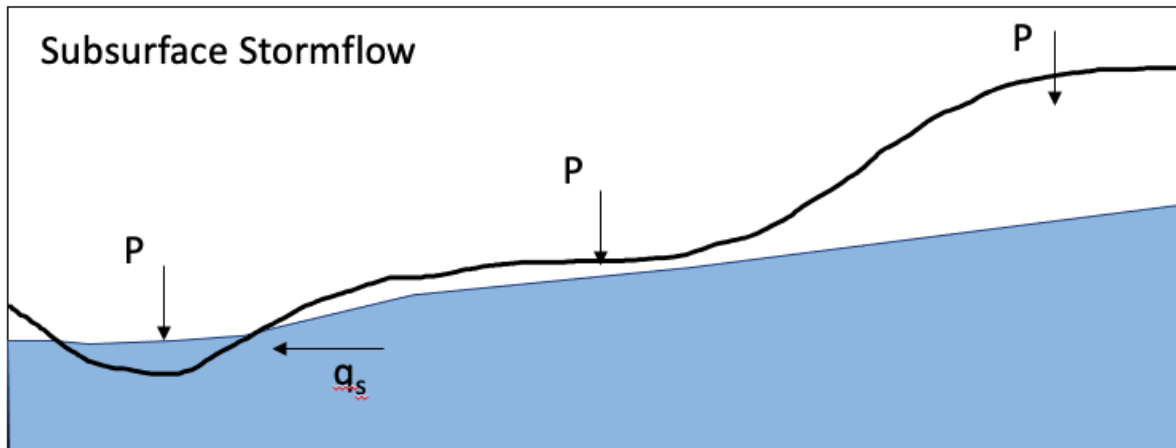
FIGURE 2: DEPICTING SUBSURFACE STORMFLOW. ARROWS INDICATING PRECIPITATION (P), AND SATURATED FLOW (Q_S). (FOLLOWING BEVEN 2000)

The third major runoff generating process is saturation-excess overland flow. The generated flow comes from two different sources, excess rain on an already saturated medium with no options but to run off, which is called ´direct precipitation on saturated areas (DPSA). The second source, return flow, occurs in sloped areas when the rate of interflow infiltration in a saturated medium upslope exceeds the capacity for interflow leaving the area by downhill subsurface flow. Runoff generated from DPSA only occur during and right after a rainfall event whereas return flow can continue to generate runoff for as long as interflow excess exists. Saturation-excess overland flow generally occurs when the soil layers have saturated to a point where no more water is able to infiltrate. This process is commonly seen during long-duration, gentle-to-moderate rainfall, with DPSA being the main process on flat areas whilst return flow being more common on sloped areas (Steenhuis et al., 2005).
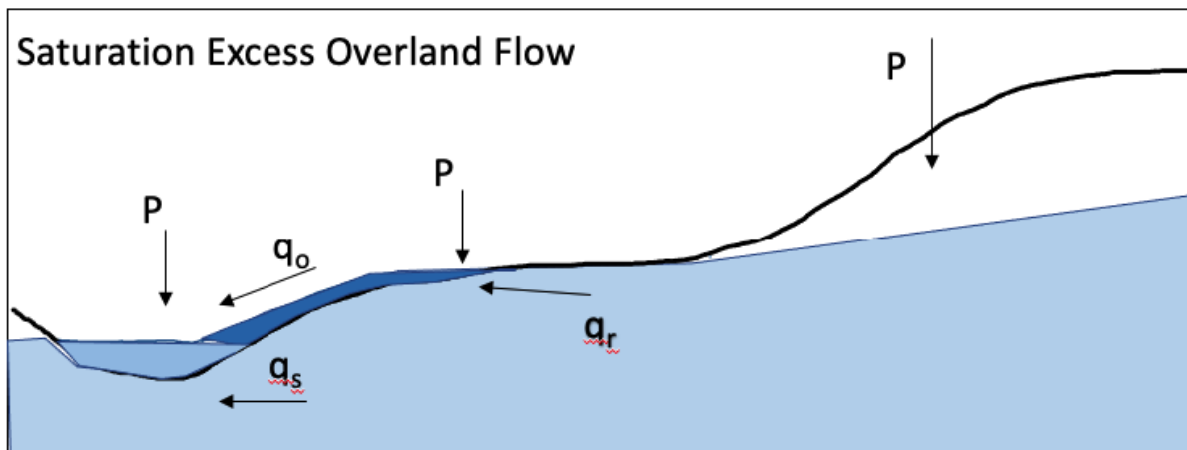
FIGURE 3: DEPICTING SATURATION EXCESS OVERLAND FLOW, ARROWS INDICATING PRECIPITATION(P), OVERLAND FLOW (Q_O), SATURATED FLOW (Q_S), AND RETURN FLOW (Q_R). (FOLLOWING BEVEN 2000)

3.7 METHODS FOR PREDICTING RUNOFF

Runoff is an essential part of the hydrological cycle and occurs as water is introduced to a system as a result of precipitation, meltwater, and other sources of flow. The impact of runoff

could not be understated as it is essential for agriculture, urban planning, industry and so forth. The ability to understand rainfall-runoff processes and incorporate them to estimate runoff generation opens up to more efficient solutions to many of the problems faced today. One of the most common ways to predict runoff is achieved through hydrological modelling, an estimation practice able to simulate continuous hydrological behaviours of a catchment area. The aim of hydrological modelling is to describe the individual flows of a hydrological system with the use of parameters controlling the magnitude of the flows and soil, topography, climate, and river properties. Due to the interaction between parameters, the accuracy of a hydrological model is highly dependent on the number of parameters included and the accurate implementation in modelling techniques with specific boundary conditions (Anees et al., 2016).

One of the earliest implementations of hydrological modelling was proposed by Mulvany in the 1850s, called "The Rational Method" (Birkel & Barahona, 2019). The Rational Method is based on a linear equation between the peak discharge (Q), drainage area (A), runoff coefficient (C), and the rainfall intensity at the time of concentration (i) and is written as:

$$Q = C * i * A \qquad\qquad (1)$$

The rational method proved to be an easy clear-cut way to simulate discharge but the limitations of the method that it could not estimate flood volume and that rainfall intensity at the time of concentration was difficult to determine proved that further improvements could be made (Shi et al., 2022). Compared to the linear equation in the rational method, the hydrological processes are highly nonlinear with complex interactions and high spatial variability. These limitations made it so the model only was physically meaningful in small impervious catchment areas in which flow could be represented as a purely kinematic process. Even with the limitations that the rational method encounter, the prediction of a hydrograph peak is still used today by engineers to design structures capable to withstand the estimated peak discharge (Beven, 2012).

3.8 EMPIRICAL HYETOGRAPHS

A hyetograph is a graphical representation of how rainfall intensity is temporally distributed. Olsson et. al. (2017) investigated the temporal distribution of heavy rain events in Sweden and in their study, a total of 2015 different rain events were extracted from historic rain data using certain criteria. The criteria follow:

1. A singular rain event is classified as an event where no previous rain was measured 1 hour before the event.
2. First and final timestep that had a mean intensity of 1/60 mm/min was identified and set as starting and ending point of an event.
3. Mean intensity was calculated for each event, if it was lower than 0.1 mm/min the event was removed due to too low intensity.
4. Any event passing the criteria above (3) was assumed a "relevant event" and events passing all the previous steps was assumed to be "extreme events".

The events were then divided into three classes dependant on duration of the event. The classes were 0-60 min, 60-90 min, and 90+ min. The classes were then grouped in five subgroups using k-means clustering on precipitation data. The k-means clustering categorize the events based

on their temporal distribution into five groups which resulted in five hyetographs representative of historic rain events in Sweden (Olsson, Berg, Eronn, Simonsson, Wern, et al., 2017).

3.9 HYDRUS 1D

Hydrus is a physically based model used to simulate the movement of water in variably saturated media. It consists of two different models, Hydrus 1D and Hydrus 2D/3D, and has a wide variety of applications. Hydrus 1D was chosen to simulate the hydrological and soil dynamic processes in this study due to its previous usage in similar projects, simplicity, and availability as a public domain model. The program uses mass-lumped linear finite element schemes to numerically solve the Richard equation (Šimunek et al., 2012).

The Hydrus 1D model describes one-dimensional water movement in incompressible, variably saturated, porous media using mass-lumped linear finite element schemes to numerically solve the Richards equation for saturated-unsaturated flow:

$$\frac{\partial \theta}{\partial t} = \frac{\partial}{\partial z}\left[K\left(\frac{\partial \theta}{\partial z} + 1\right)\right] - H \tag{1}$$

K is the unsaturated hydraulic conductivity, θ is the water content in the soil, z is the vertical coordinate positive upwards, and H is a sink term representing the evapotranspiration and root uptake (Broekhuizen et al., 2021).

The model then uses van Genuchten equations to set the initial water retention curve $\theta(h)$ which relates volumetric water content in pressure potential to hydraulic conductivity $K(h)$. Hydrus 1D have plenty of ways to simulate this but the van Genuchten-Mualem model was chosen in this study due to its previous application in similar experiments (Caiqiong & Jun, 2016; Wang et al., 2022). The van Genuchten-Mualem model models the variation in hydraulic conductivity (K_h) with soil moisture content where:

$$\theta(h) = \begin{cases} \theta_r + \dfrac{\theta_s - \theta_r}{[1 + |\alpha h|^n]^m}, & h < 0 \\ \theta_s & h \geq 0 \end{cases} \tag{2}$$

$$K(h) = K_s S_e^l \left[1 - \left(1 - S_e^{\frac{1}{m}}\right)^m\right]^2 \tag{3}$$

Where the effective saturation (S_e) is

$$S_e = \frac{\theta - \theta_r}{\theta_s - \theta_r} \tag{4}$$

$$m = 1 - \frac{1}{n}, n > 1 \tag{5}$$

In equation (2) *h* represents the water pressure head, θ_s is the saturated soil water content, θ_r is the residual soil water content, K_s represents the saturated hydraulic conductivity. α, *l*, and *n* affects the shape of the soil water retention curve, from which α denotes the inverse of the air entry value, l relates to the pore-connectivity of the soil, and n represents a pore-size distribution index (Wang et al., 2022).

The soil hydraulic parameters given in equation (2) are possible to measure in a laboratory or in field. However, the standard practice measurements are often very time consuming and elaborate and would not fit the scope of this study. This was avoided by using a built-in model called Rosetta to predict these parameters using more trivial values such as bulk density and soil texture. Rosetta is based on neural network analysis that implements five hierarchical pedotransfer functions (PTF) to estimate the van Genuchten water retention parameters seen in equation (2). Rosetta's usage in previous studies is well recorded but it should be taken into account that the generated values are estimations and will most likely differ from actual empirical values (van Genuchten et al., 2001)

The four parameters required to achieve the highest accuracy from the Rosetta model were soil texture in percentage of clay, silt, and sand, bulk density, and water retention at 330 cm and 15 000 cm (wilting point) (Shaap et.al 2001). Rosetta is also able to estimate infiltration capacity from these parameters and could be used as comparison to field values.

An important parameter for the water cycle in the upper layers that Hydrus is able to estimate is the reference evapotranspiration (ET_0) which is the combined evaporation and transpiration for a reference surface, in this case grass. Hydrus offers two different formulas to calculate the reference evapotranspiration, the Hargreaves equation, which is an empirical approximation only requiring data of the air temperature, written as:

$$ET_0 = 0.023(0.408)(T_{mean} + 17.8)((T_{max} - T_{min})^{0.5} * R_a) \tag{6}$$

Where T_{max} = maximum air temperature (˚C), T_{min} = minimum air temperature (˚C), T_{mean} = mean daily temperature (°C), R_a = extraterrestial radiation (MJ/m^2). The Hargreaves equation comes with greater inaccuracy but can still be used when available meteorological data is insufficient.

The second option to approximate the reference evapotranspiration is the Penman-Monteith equation. Penman-Monteith is a physically based approach and is recommended by organisations such as The Food and Agricultural Organisation of the United Nations (FAO) as the standard method for determining reference evapotranspiration. The equation is written as:

$$ET_0 = \frac{0.408\Delta(R_n - G) + \gamma\frac{900}{T+273}\mu_2(e_s - e_a)}{\Delta + \gamma(1 + 0.34\mu_2} \tag{7}$$

Where *T* = mean air temperature (˚C), μ_2 = wind speed (m/s), R_n = Net Radiation Flux (MJ/m^{2}day), *G* = sensible heat flux into the soil (MJ/m^{2}day), e_s = mean saturation vapor pressure (kPa), e_a = mean ambient vapour pressure (kPa), γ = psychrometric constant (kPa/˚C), Δ = slope (first derivative of the function (*eT*)). The issue that comes with the Penman-Monteith

equation is that it requires various meteorological parameters which could be difficult to acquire for site specific experiments (Berti et al., 2014).

4. METHOD

4.1 PRE-STUDY

A pre-study was conducted to find a suitable soil model that could simulate the sought after hydrological and soil dynamic processes. This was done by searching in the database Science Direct using the search terms "Soil Moisture" and "Precipitation" and "Model".

A literature study followed to give background and context to the thesis. The literature study focused on previous research on modelling techniques simulating historic rain events and the different hydrological processes precent. Furthermore, the study included main runoff mechanisms in different soils and topography. The complete literature study was conducted using Science Direct with the search terms: "Model" and "Precipitation" and "Soil Moisture", "Antecedent Wetness" and "Simulation" and "Historic Rain Event", "Soil Features" and "Sweden", "Green Urban Areas" and "Sweden" and "Hydraulic Conductivity".

4.2 STUDY SITE

This study was conducted in Uppsala municipality in Sweden where three different study sites were chosen. The sites were chosen due to them being green urban areas in close proximity to the city centre. The first study site, marked as 1 in Figure 4, was located just outside Geocentrum in a green area used for recreational activity. The area was mainly grass-covered with some larger trees nearby and was surrounded by paved roads. The green area had some difference in topography; however, a mostly flat surface was chosen for this study. The main soil type was identified using the Sveriges geologiska undersökning © (SGU) Jordartskarta and was determined to consist of glacial clay (Sveriges Geologiska Undersökning, n.d.).

The second study site, marked as 2 on Figure 4, was located in Artilleriparken close to BMC. This site was a flat grass covered area close to several residential buildings and had little to no change in topography. Running through the area was also a well-trafficked gravel cycle-road in connection to Uppsala universitet. The main soil type was identified as sand with the SGU Jordartskarta.

The third and final study site, marked as 3 on Figure 4, was located on a large grassy area in southern Uppsala near the Ångströms laboratory. The location had forested areas to the north and south, and the highly trafficked Dag Hammarskjöld's Väg to the west, and residential buildings to the east. The main soil type identified using SGU's Jordartskarta was glacial silt.
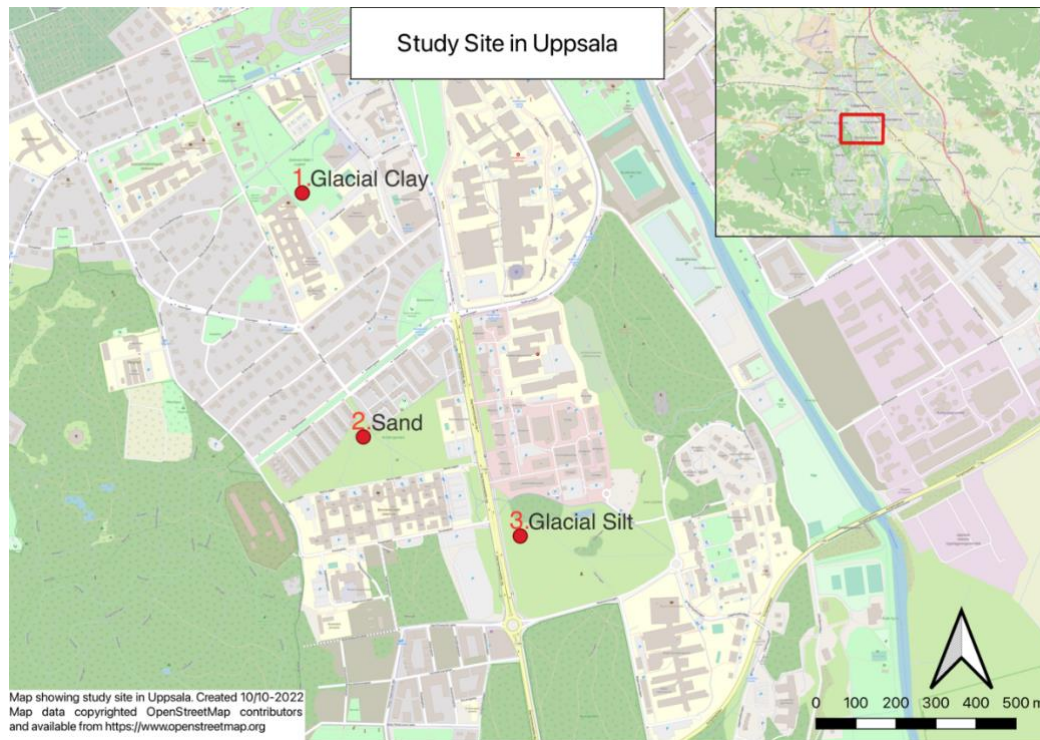
FIGURE 4: MAP SHOWING THE THREE STUDY SITES IN UPPSALA, SOIL TYPE IDENTIFIED WITH SGU JORDARTSKARTA INCLUDED IN TEXT

4.2.1 EXPERIMENTAL SET-UP

The field experimental set up consisted of a double ring infiltrometer with diameters 30 and 20 cm with a height of 20 cm. These rings were hammered down using a hammer and a small amount of water was poured into the rings to ensure there was no leakage from the rings. Once this had been determined a ruler was placed inside the inner ring and water was poured into the rings until they were full. Filling up the rings had to be done carefully to not damage the topsoil structure. Once the rings were full, a timer was started, and measurements of the water level were noted down at increments depending on the infiltration speed. The measurements stopped once a constant stable infiltration capacity was reached.

While the infiltrations measurements were taken, up to three 40 cm deep holes were dug around the experiment to investigate the soil structure on the site. Pictures were taken of the soil profile and soil samples were taken in the holes. If the profile of two holes were deemed to display different characteristics, a third hole was also dug. Two soil samples were then taken in each hole, preferably one in each layer, but if no layers could be seen by the naked eye, the samples were taken at 10 respectively 30 cm. The samples were taken using metal soil sample containers that were pushed into the soil profiles. The containers were then dug out from the hole and placed in sealed plastic bags to be brought back to the laboratory.

FIGURE 5: EXPERIMENTAL SETUP ON SITE 2, DOUBLE RING INFILTROMETER CAN BE SEEN IN THE CENTRE OF THE PHOTO, THE YELLOW CYLINDER BELOW WAS USED TO TAKE SOIL SAMPLES

4.2.2 FIELD MEASUREMENTS

A field experiment was set up to determine the parameters required for the Rosetta model in three different soils. The soils were chosen from their soil texture to include one sandy, one clayey, and one silty soil. This was done to investigate a broader spectrum of representative soils for different regions in Sweden.

The soil texture was determined with the Jar-test, where a soil sample was sieved through a 2 mm sieve and mixed with water under heavy stirring to destroy any aggregate structures present in the soil. The mixture was then left to sit for 24 hours so the soil could sediment. Once all the soil had sedimented properly, the layering of the soil could be determined with the densest particles gathering at the bottom. A ruler was then used to measure the different layers with sand at the bottom, silt in the middle, and clay at the top.

To determine the bulk density of the soil, the core cutter method was chosen. A cutter with the diameter 8 cm and height 5 cm was hammered into the soil and dug out. A straight edge knife was then used to trim down the sample to perfectly fit the cutter, the cutter was then placed in a sealable plastic bag to ensure no moisture evaporated. The sample was then brought to the lab and weighted before it was dried at 105 °C. To ensure all moisture had evaporated the cutter was dried for 24 hours. The dry sample was then weighted, and the bulk density calculated with equation (6)

$$BD = \frac{mass\ dry\ soil}{volume\ of\ core} \qquad (6)$$

The infiltration capacity was measured using a ring infiltrometer which measures the amount of water that infiltrate the soil surface by measuring how fast the water level in the ring decreases. A problem with this method is that it tends to overestimate the infiltration capacity due to flow of water in the soil profile is not purely vertical but instead tend to diverge horizontally. This happens due to capillary forces in the soil that pulls the infiltrated water to the sides, allowing more water to infiltrate. This process does not accurately represent a rain event as only a very small area is subjected to water. A way to overcome this problem was to use a double ring infiltrometer (figure 6) that adds an outer ring that was filled with water to create a wetting front outside the inner ring. This ensured that the infiltrated water mainly moves vertically and further increases the accuracy of the measurement (Gregory et al., 2005). The outer ring was constantly filled with water so that a constant water level remained throughout the experiment. The outer ring of the double infiltrometer available had a diameter of 60 cm and a height of 20 cm, and the inner 30 cm with a height of 20 cm. To ensure that the outside ring created a completely saturated front, the ring should be filled up 4-8 times for each experiment. This deemed to be unpractical due to the amount of water needed to complete the experiment (>1 ton). Instead, a makeshift inner ring was made from a PVC-tubing with the diameter of 15 cm. By reducing the diameter of the double ring infiltrometer the accuracy of the measurement also decreased due to a bigger risk of lateral flow, however this was considered necessary due to the logistics. Yolcubal et. al. (2004) mentions that a commonly used dimension for the double ring infiltrometer is 30 cm diameter which would indicate a good-enough accuracy for the measurements in this study.
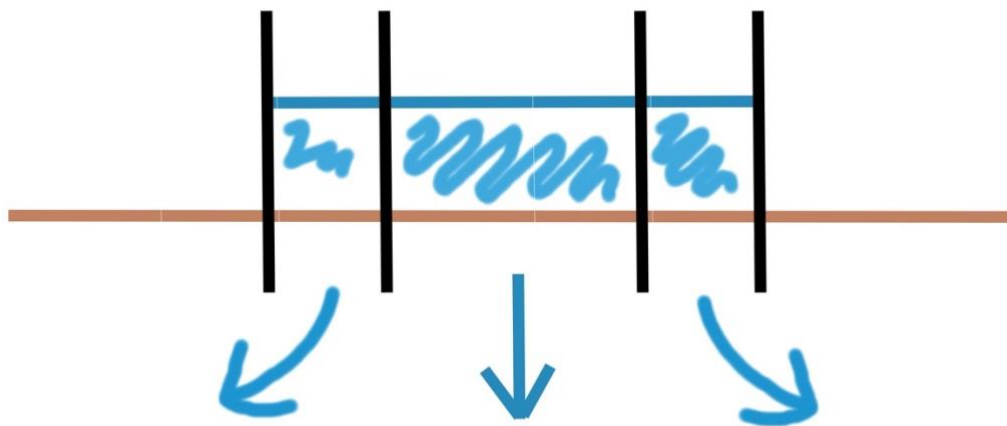
FIGURE 6: SIDE VIEW OF A DOUBLE RING INFILTROMETER

Investigating the water retention at 330 and 1500 cm suction was at first considered in this experiment to achieve the highest accuracy of the Rosetta model. This was supposed to be measured with a pressure plate apparatus. The procedure was later determined to be too time consuming to fit in the scope of this study and therefore bulk density and soil percentages were used as input parameters.

4.3 MODEL SETUP

Hydrus-1D offers a large variety of settings and equations to estimate site specific features, such as crop data and heat transport. The main processes included in the hydraulic model for this experiment was water flow, governed by the Richard's equation, and a root water uptake model. The soil profile was set to a depth of 40 cm containing an upper layer spanning from 0 – 20 cm and a lower layer from 20 – 40 cm. Values from the field experiment and the Rosetta model were put in each layer. Van Genuchten-Mualem single porosity model was chosen to represent the soil hydraulic process under the assumption that no major differences in hydraulic permeability between the two layers and only mobile flow regions are present in the soil. The total simulation time for the model added up to 27 years, with the two first years repeated and used to warm up the model to set up initial conditions. The Penman-Monteith equation was chosen to represent the potential evapotranspiration (ET_0) and daily meteorological values from SMHI was used as input together with values generated from the Hydrus database (Allen et.al 1998). Grass was chosen as the vegetation on the sites, the crop height was set at 10 cm and root depth 10 cm. The leaf area index was generated for crop height of clipped grass from the Hydrus database. Regarding the root water uptake model, the governing equation chosen was the Feddes reduction function, that incorporates a water stress function to crops related to pressure heads. The parameters required for the Feddes function for grass were retrieved from the Hydrus database. To investigate how the soil moisture changes throughout the soil profile, five observation points were inserted at depths 0, 10, 20, 30, and 40 cm.

4.4 BOUNDARY CONDITIONS

Simulating water flow in Hydrus-1D requires an upper boundary condition (BC) as well as a lower boundary condition. The upper BC used is this study was "Atmospheric BC with surface runoff". This BC incorporate climatic conditions like precipitation, evaporation, and root uptake that switches the BC from a flux BC to a pressure head BC when the specified flux into the soil is higher than the infiltration capacity of the soil. The pressure head at the boundary becomes zero once this happens and all excess water is removed as surface runoff. For the bottom BC, "Free Drainage" was chosen under the assumption that the water table never reaches the soil profile. Free Drainage specifies a unit total gradient at the boundary of the soil profile and that the flow is gravity flow with the pressure head gradient being zero.

4.5 CLIMATE DATA

Meteorological data of precipitation, wind speed, relative humidity, temperature, and radiation was gathered from the Sveriges Meteorologiska och Hydrologiska Institut (SMHI)'s data base. The data was mainly gathered from the same station but due to incomplete data series some data had to be sourced from nearby stations. Precipitation data was given in 15 minutes increments whilst daily values were given for the rest of the data. Stations Adelsö A and Tullinge A in Stockholm was chosen for the climate data as no stations in Uppsala had sufficient data and was assumed to also be representative of precipitation in Uppsala. Daily precipitation data was also available but due to finer temporal resolution is considered to better represent rainfall events the 15-minute data was chosen for the simulations (Berne et.al 2004). Most of the retrieved data series had gaps with missing values and to be able to get a complete time

series some of the values had to be interpolated. Linear interpolation was chosen as the method to retrieve the missing values, but since the precipitation data did not include values below 0.1 mm interpolated values would break this trend and might add values in cases no precipitation was recorded. Therefor values from a nearby station were used to fill in the missing precipitation values.

4.6 MODEL STRATEGY

In this study, two different types of rain events forced the Hydrus-1D to investigate the relation between soil moisture, runoff, and precipitation. The simulations were applied to the three different soils investigated in the field experiment with the only difference being how precipitation was modelled and what temporal scale was used.

4.6.1 HISTORIC SIMULATION

The first simulation was modelled using historic climate data from a 25-year time series spanning from 1st January 1997 to 1st January 2022. This period was chosen due to the heat transport in Hydrus should preferably start at the beginning of the year. The aim of the simulation was to further investigate the soil moisture dynamics by extracting data at the start of heavy rainfall events and by analysing the dynamics of soil moisture, precipitation, and surface runoff over time. A further analysis was conducted on the correlation between event total precipitation amount, precipitation intensity, precipitation duration, and antecedent soil moisture to investigate the main driving force for runoff generation on the studied sites.

To be able to extract the rain events from the time series they first must be defined as singular rain events. This was done using the same definition as Ico Broekhuizen used in his study investigating difference in urban drainage models and their effects on simulated runoff. Broekhuizen defined a rain event as a "*minimum 3-hour antecedent dry weather period, as well as a total depth of at least 2 mm and an average intensity of at least 0.01 mm/h* "(Broekhuizen et al., 2019, p.4). The definition for a singular rain event was also limited to months April-October to ensure snow-free conditions. The median soil moisture at depths 10, 20, 30, 40 cm was used as initial condition for the following simulations.

4.6.2 HYETOGRAPH SIMULATION

The second part of the simulations consisted of rain events represented as five different hyetographs based on the study by Olsson et al. (2017). These rain events were only simulated on Site 1 to fit the results within the time scope of this study.

Myndigheten för samhällsskydd och beredskap (MSB) recommends a duration of a couple of hours for events when simulating surface runoff in urban areas, therefore the hyetographs representing long events (90+ min) were used (MSB, 2017). The length of the event was set to 120 minutes with an average intensity of 32.6 mm/h and a total precipitation amount of 65.2 mm. The total rain amount used in the hyetographs was put to represent a rain event with the return period of 100 years due to this return period historical relation to floodings in Sweden (MSB (Swedish Civil Contingencies Agency), 2012). The average intensity was calculated

using an IDF-curve that incorporated local conditions in Sweden. The hyetographs presented in figure 7 show the temporal variation of precipitation intensity for each event.
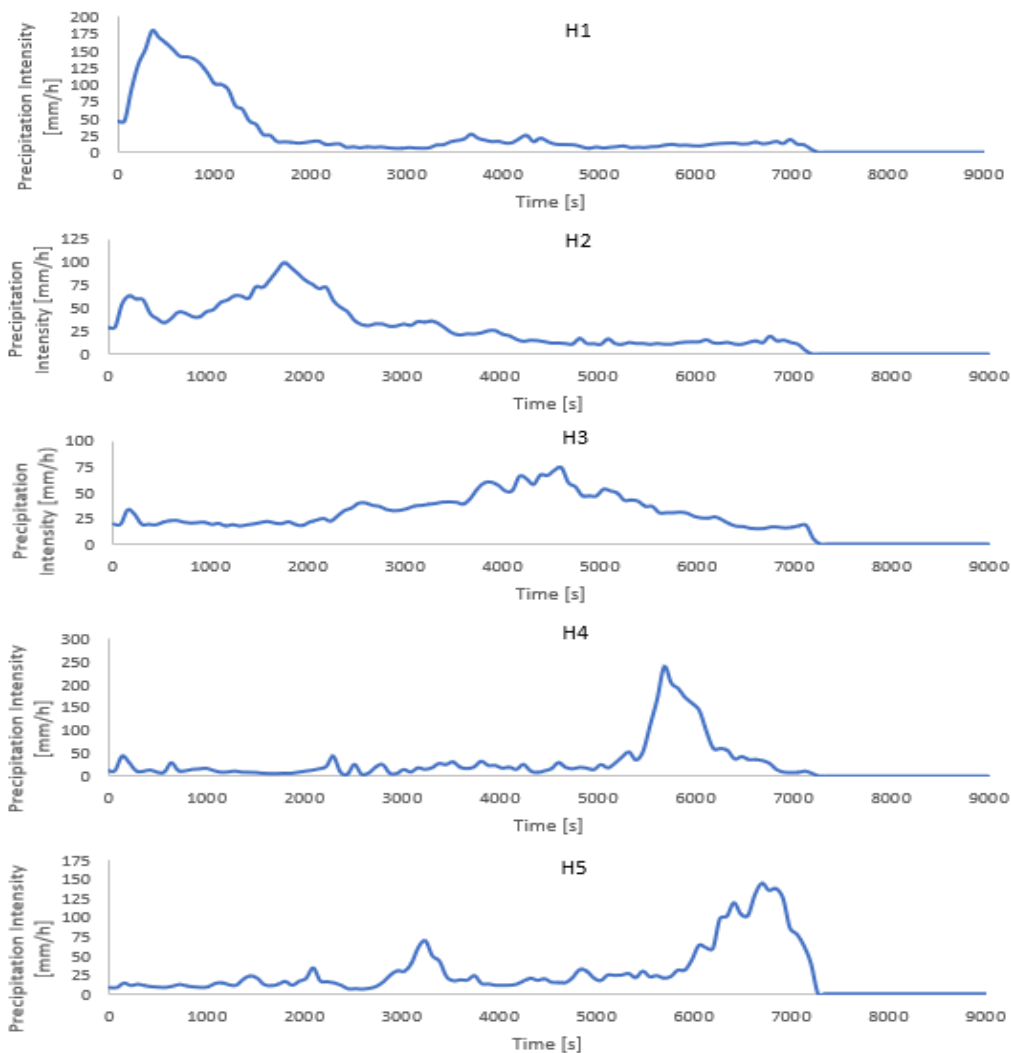
FIGURE 7: HYETOGRAPHS 1 -5 REPRESENTING INTENSE RAINFALL EVENTS IN SWEDEN, SOURCED FROM OLSSON (2017)

4.7 COEFFICIENT OF DETERMINATION

To determine how well two parameters relate to each other the coefficient of determination, or R^2-value, will be used as an indicator. R^2 is a measurement that is used to determine the goodness of fit in a linear regression model. Values closer to 1 indicates a strong significant linear relation between parameters. R^2 is the square of the correlation coefficients of the variables present in the linear regression model (Cheng & Garg 2014).

4.8 MULTIPLE LINEAR REGRESSION

To investigate the first two research questions a multiple linear regression (MLR) analysis was conducted on the parameters determining runoff generation. The MLR used was of the type ordinary least squares with the dependent variable runoff, the independent variables were event total precipitation amount, mean precipitation intensity, peak 15 minutes precipitation intensity,

antecedent soil moisture, and precipitation duration for the historic series. The MLR was conducted using the statsmodels-package in python.

5. RESULTS

5.1 SOIL SAMPLES IN THE FIELD

The first site had a sparse vegetation cover mainly consisting of grass. The site was on a flat spot downhill from a paved road and hills, in combination of Uppsala recently experiencing rainy days had made the site quite wet. The presence of earthworms was also noted, and wormholes could be easily seen in the profile. The bottom layer from 20-40 cm was more tightly packed than the upper layers but also showed presence of wormholes. Three different holes were dug, and all the soil profiles showed similar features such as a clay layer, one of the holes had a slightly light-coloured clay in comparison. The soil samples were taken at depths 10 and 30 cm.

The second site had a much thicker vegetation cover with longer grass, approximately 20 cm tall. The site was on a flat spot in the middle of a green area with little construction nearby. A lot of macropores were present in the soil. The soil profile did not show any clear signs of layering and the colouration of the soil remained constant throughout the profile. For this reason, only two holes were dug at this site and samples were taken at depths 10 and 30 cm.

The third and final site, Ångströms, had a vegetation cover of grass and moss. The grass looked as if it had recently been cut by some heavy machine that had left tracks at the site. The roots reached 10 cm down the profile and no earthworms was seen during the experiment. The site was also the driest of the three and the soil profile showed clear signs of layering. The upper part of the layer looked like a mixture of sand and silt but deeper in the profile a layer of light-coloured sand could be clearly seen. Three holes were dug at this site and samples were taken of the two different layers, one at 20 cm and another at 35 cm to include some of the light-coloured sand.

The results from the Jar-test showed that the three different sites had varying soil textures in the lower layer, the upper layers showed more similarities to each other. Sand was the most prevalent fraction in all studied soils, followed by silt and clay. Table 1 shows the texture of the upper and lower layer of the soils, classification according to the soil texture triangle is also included.

TABLE 1: RESULTS FROM THE JAR-TEST DEPICTING TEXTURE CLASS OF LAYERS AT THE SITES

Sample	% Clay	% Sand	% Silt	Soil Texture Triangle
Upper Site 1	2,63	79,31	18,06	Loamy Sand
Upper Site 2	3,63	75,91	20,46	Loamy Sand
Upper Site 3	0,87	90,30	8,84	Sand
Lower Site 1	36,44	47,97	15,59	Sandy Clay
Lower Site 2	4,95	63,16	31,88	Sandy Loam
Lower Site 3	2,00	89,24	8,75	Sand
Average Site 1	19.53	63,64	16,82	Sandy Clay Loam
Average Site 2	4,30	69,53	26,17	Sandy Loam
Average Site 3	1,43	89,78	8,80	Sand

The first site contained the largest fraction of clay in the lower layer and was considered a sandy clay, the upper layer was considered a loamy sand. Site 2 had the largest fraction silt, both in the upper and lower layer. Site 2 was considered loamy sand in the upper layer and sandy loam in the lower layer. The soil type of site 3 was determined to be sand in both layers, showing very small fractions of clay and silt.

The obtained bulk densities from the core cutter method are shown in Table 2. From the results the bulk density in each of the sites were quite similar, varying less than 0,1 g/cm^3 for all the layers. Site 3 had the highest bulk density for both the layers, followed by Site 2 and lastly Site 1.

TABLE 2: BULK DENSITY OF THE UPPER AND LOWER LAYERS OF THE THREE SOILS

Site	Bulk Density (g/cm^3)
Upper Site 1	1,275
Upper Site 2	1,285
Upper Site 3	1,340
Lower Site 1	1,262
Lower Site 2	1,290
Lower Site 3	1,322

The results show a relation between lower bulk density and clay content, the layer with the lowest bulk density had the highest clay content. It also showed that having a high sand content could indicate a higher bulk density. Although small, all the measured sites showed a difference between the layers, with the upper layer having a higher bulk density than the lower layer. This goes against the general assumption that bulk density increases with depth in a soil profile. The reason probably being that the investigated green areas have had its upper layers replaced with a topsoil better suited for vegetation.

The results from the double ring infiltrometer test showed varying result. The infiltration capacity was lowest at Site 1, followed by Site 2, and lastly Site 3. Two measurement was conducted on Site 1 and 2, whilst only one measurement was made on Site 3.

Figure 8 shows the average infiltration capacity on Site 1, the measurement went on for 77 minutes but showed a constant infiltration rate about halfway through the experiment. The relatively low infiltration capacity was possibly due to the high amount of clay seen in the soil.
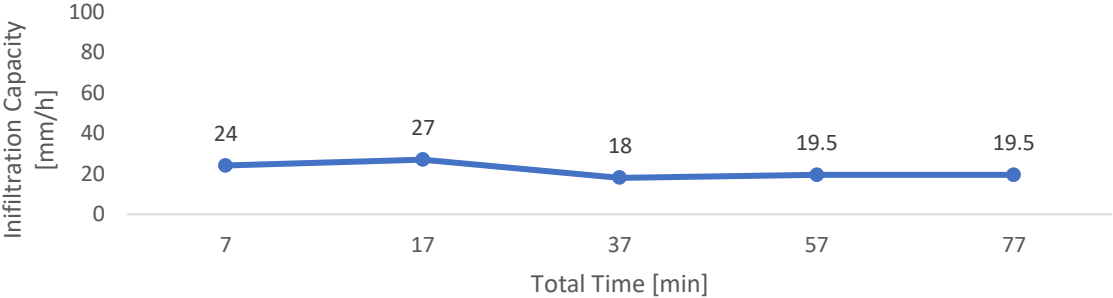
FIGURE 8: AVERAGE INFILTRATION CAPACITY AT SITE 1

Figure 9 shows the infiltration capacity at site 2, the measurements were taken for 60 minutes and showed a constant infiltration rate about halfway into the experiment. The infiltration capacity was three times higher than what could be seen at Site 1, this was probably due to it containing less clay, but also due to the presence of more macropores.
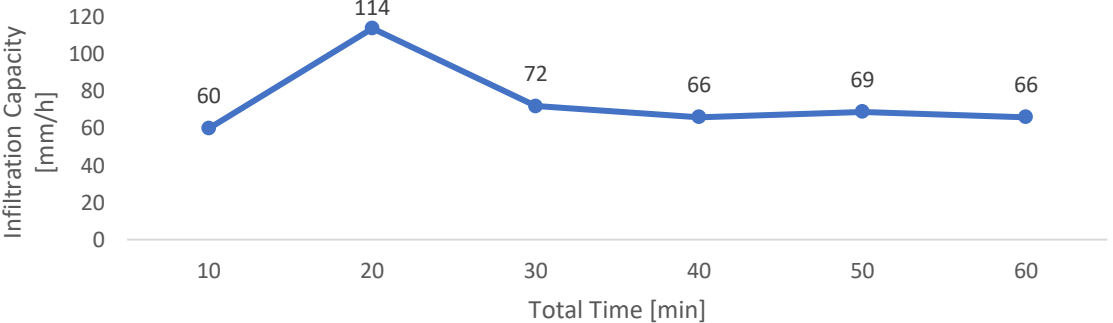
FIGURE 9: AVERAGE INFILTRATION CAPACITY AT SITE 2

Figure 10 shows the infiltration capacity on Site 3. For this experiment the infiltration capacity of the soil was so high that the water supply ran out after 18 minutes of measuring. The infiltration capacity on Site 3 was ten and thirty times higher than what was recorded at Site 2 and 1, the reason probably being due to large percentage of sand in the soil. The final infiltration capacity could not be verified with certainty due to only one measurement being taken. However, the measurement that was made showed that the experiment reached a constant infiltration rate, so the results were deemed to be accurate enough to use in this study.
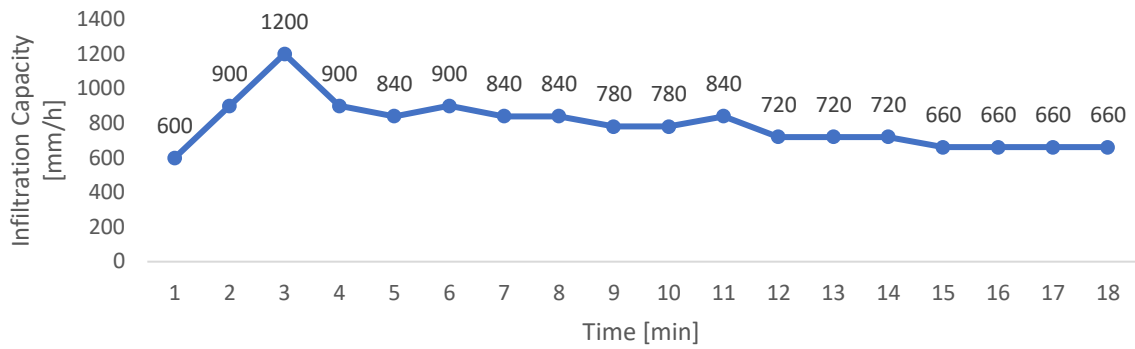
FIGURE 10: AVERAGE INFILTRATION CAPACITY AT SITE 3

Figure 11 shows a comparison of the measured empirical values from the field experiment and the generated values from Rosetta's neural network. The results show that the neural network overestimates values for the finer coursed soils in Site 1 and 2 and underestimate the values in the courser soil in Site 3. Due to the limited amount of data gathered, the values from the Rosetta model could not be confirmed to represent the soils in this study. Therefore, the empirical data for infiltration capacity gathered at the sites were used for the simulations.
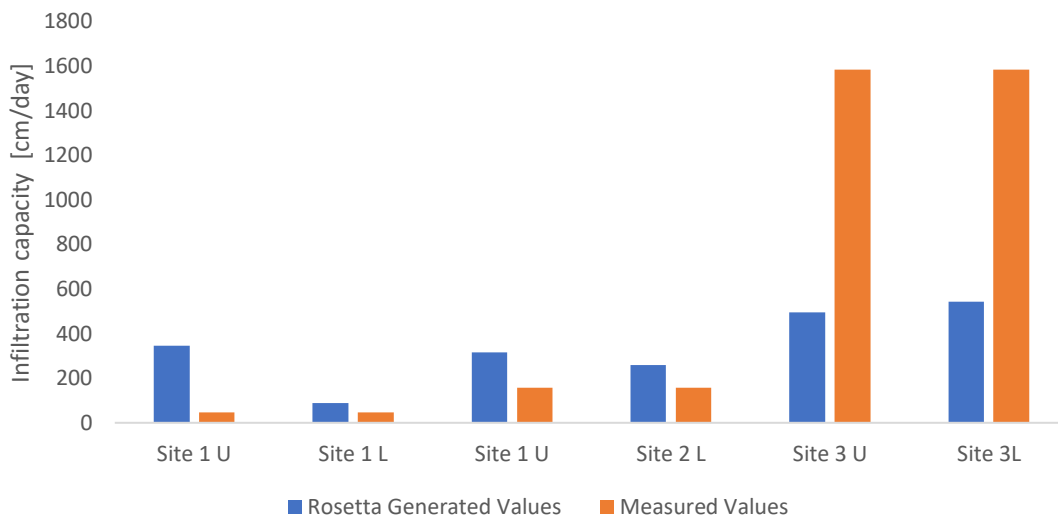
FIGURE 11: GENERATED VALUES AND MEASURED VALUES FOR INFILTRATION CAPACITY, U REPRESENTS UPPER LAYER, L REPRESENTS LOWER LAYER

5.2 HISTORIC RAIN SIMULATION

The historic rain simulation in Hydrus 1D simulated precipitation from a 25 year long data series recorded in Stockholm on three different soils. The purpose of this simulation was to investigate the relation between generated surface runoff, precipitation, and soil moisture. A total of 1307 singular events were extracted from the historic series using the definition explained in chapter 4.6.1.

Out of the three soils, surface runoff was generated on Site 1 and Site 2. Site 3 showed no signs of any surface runoff generation during the entire simulation period. Surface runoff was generated on Site 2 two times during the simulation period and 12 times on Site 1. Total

precipitation, peak precipitation rate and total runoff amount from Site 1 is presented in table 3 and from Site 2 in table 4.

TABLE 3: TOTAL PRECIPITATION, PEAK PRECIPITATION, AND TOTAL SURFACE RUNOFF AMOUNT FOR EVENTS THAT GENERATED RUNOFF FROM THE HISTORIC RAIN SIMULATION ON SITE 1

Total Precipitation (mm)	Peak Precipitation (mm/h)	Total runoff amount (mm)
33.6	80,4	10,85
47.9	62,4	9,6
36.4	40,8	4,6
66.9	33,6	3,4
33.4	48	3,3
19.5	40	2,4
23.5	28	1,2
39.7	33,6	1,1
29.9	23,2	0,8
25.4	29,6	0,4
33.7	36,4	0,4
82.7	20,4	0,2
20.9	44,4	2

TABLE 4: TOTAL PRECIPITATION, PEAK PRECIPITATION, AND TOTAL SURFACE RUNOFF AMOUNT FOR GENERATED RUNOFF FROM THE HISTORIC RAIN SIMULATION ON SITE 2

Total Precipitation (mm)	Peak Precipitation (mm/h)	Total runoff amount (mm)
33,6	80,4	0,11
47,9	62,4	0,02

To investigate the main driving force for runoff generation on the event total precipitation, duration, and intensity was plotted against the generated runoff (Figures 12-14). To graphically investigate the impact from antecedent soil moisture on surface runoff, three different classes of soil moisture were set. The classes are representative of the soil moisture values in the 33 percentiles, values in between the 33 and 66 percentiles, and values above the 66 percentiles. Soil moisture values corresponding to classes are presented in table 5 and the wilting point, field capacity and value for full saturation are presented in table 6.

TABLE 5: THE DISTRIBUTION OF THE THREE SOIL MOISTURE CLASSES, THETA (Θ) REPRESENTS THE VOLUMETRIC SOIL MOISTURE CONTENT (CM³/CM³)

Antecedent soil moisture (%)	28>Θ	28≤Θ<33	33≤Θ
Class	1	2	3

TABLE 6: WILTING POINT, FIELD CAPACITY, AND SATURATION POINT FOR EACH SITE, THETA (Θ) REPRESENTS THE VOLUMETRIC SOIL MOISTURE CONTENT (CM³/CM³)

	Wilting Point (Θ)	Field Capacity (Θ)	Saturation (Θ)
Site 1	0,10	0,28	0,51
Site 2	0,06	0,20	0,43
Site 3	0,04	0,14	0,3

Figure 12 shows the relation between precipitation amount and runoff generation. It achieved a determination coefficient of R² = 0,0157, which wouldn't indicate a significant relation between the parameters. However, it does give an indication of a threshold that shows that the amount of precipitation required to generate runoff on Site 1 cannot be lower than 20 mm. Another noteworthy takeaway from figures 12-14 is that runoff rates above 0,4 mm/h were only achieved in combination with an antecedent soil moisture of at least class 2.
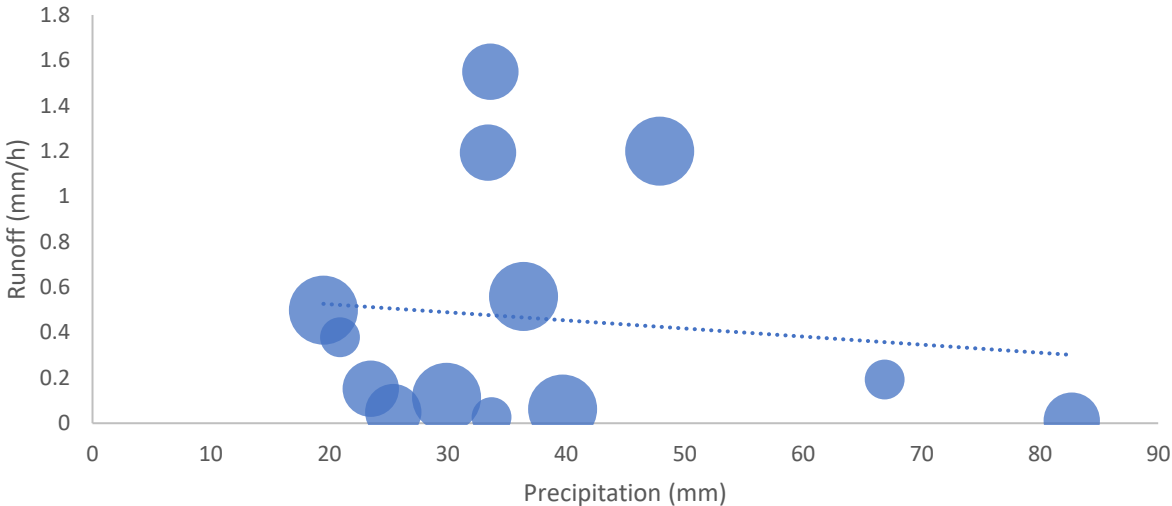
FIGURE 12: SHOWS THE RELATION BETWEEN EVENT TOTAL PRECIPITATION AMOUNT AND GENERATED RUNOFF. THE SIZE OF THE CIRCLES REPRESENT THE SOIL MOISTURE CLASS, CLASS 1 IS THE SMALLEST CIRCLE, CLASS 2 THE MEDIUM CIRCLES, AND CLASS 3 THE LARGEST CIRCLE

Figure 13 shows the relation between runoff generation and rain duration. The two parameters do not show any clear sign of correlation, but the input trendline does show a slight negative trend with a correlation coefficient of R² = 0,3003. The figure also shows that the only rain events that generated runoff above 0,2 mm/h had a duration shorter than 9 hours, with the highest runoff generation being achieved at a duration of 7,5 hours.
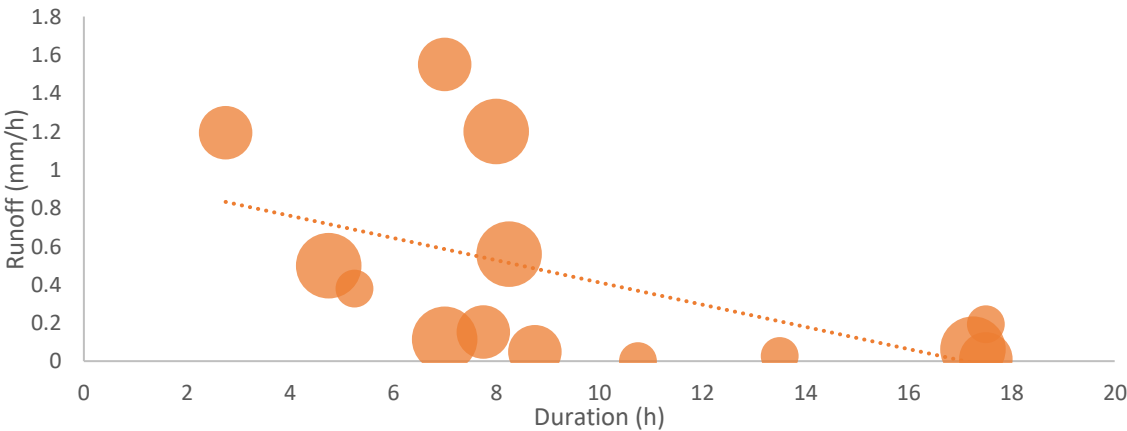
FIGURE 13: SHOWS THE RELATION BETWEEN PRECIPITATION DURATION AND RUNOFF GENERATION. THE SIZE OF THE CIRCLES REPRESENT THE SOIL MOISTURE CLASS, CLASS 1 IS THE SMALLEST CIRCLE, CLASS 2 THE MEDIUM CIRCLES, AND CLASS 3 THE LARGEST CIRCLE.

Figure 14 shows the relation between precipitation intensity and runoff generation. The precipitation intensity achieved the highest R^2-value (0,408) plotted against runoff generation of the three investigated parameters. The figure shows a slight positive trend as runoff generation increases with precipitation intensity. It can also be seen from the figure that for runoff generations higher than 0,4 mm/h, the required intensity on Site 1 was at least 4 mm/h.

The precipitation intensity of the rain events achieved the highest correlation with runoff generation of the investigated parameters, but the relation was still uncertain due to the low R^2-value. Therefor a further investigation on the parameters included in precipitation intensity was conducted. Due to the used definition for a rain event, the temporal variation of rainfall intensity during an event was not included in figure 14, and a mean value for the precipitation intensity was used to represent the event. Therefore, the investigated parameter was chosen to be peak 15-minute precipitation intensity, the maximum intensity during the rain event.
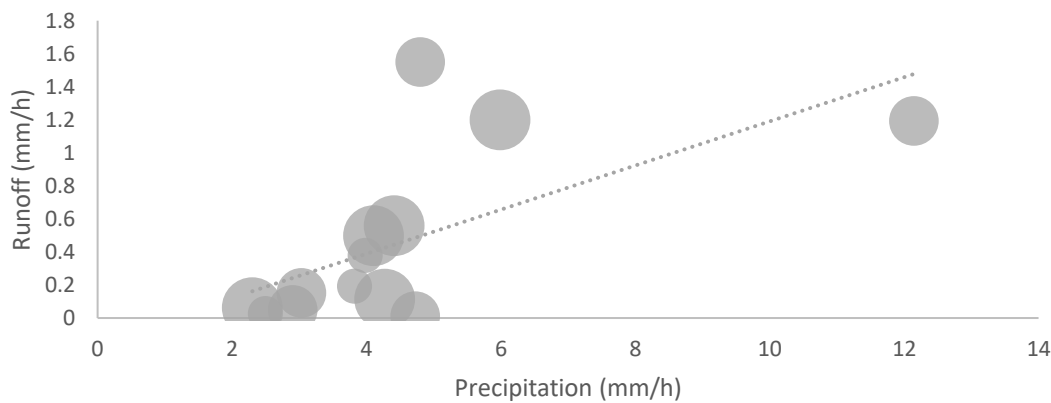
FIGURE 14: SHOWS THE RELATION BETWEEN PRECIPITATION INTENSITY AND RUNOFF GENERATION. THE SIZE OF THE CIRCLES REPRESENT THE SOIL MOISTURE CLASSES, CLASS 1 IS THE SMALLEST CIRCLE, CLASS 2 THE MEDIUM CIRCLES, AND CLASS 3 THE LARGEST CIRCLE

Figure 15 shows the relation between the runoff generation and peak precipitation. The peak precipitation intensity seems to have a strong effect on the generated runoff in comparison to the other investigated parameters. The relation achieved a determination coefficient of $R^2 = 0,8552$ which indicates a strong relation between the parameters. The highest runoff generation was achieved during a peak rain intensity of 80,4 mm/h, and for runoff generations higher than 0,2 mm/h, a peak intensity of 40 mm/h was required on Site 1. Also noteworthy is that runoff only was generated when the precipitation intensity was greater than the soil hydraulic conductivity.

The amount of runoff generated on Site 2 was considered to be negligible due to the very low amount and therefore the initial conditions for the hyetographs were set using values from Site 1.
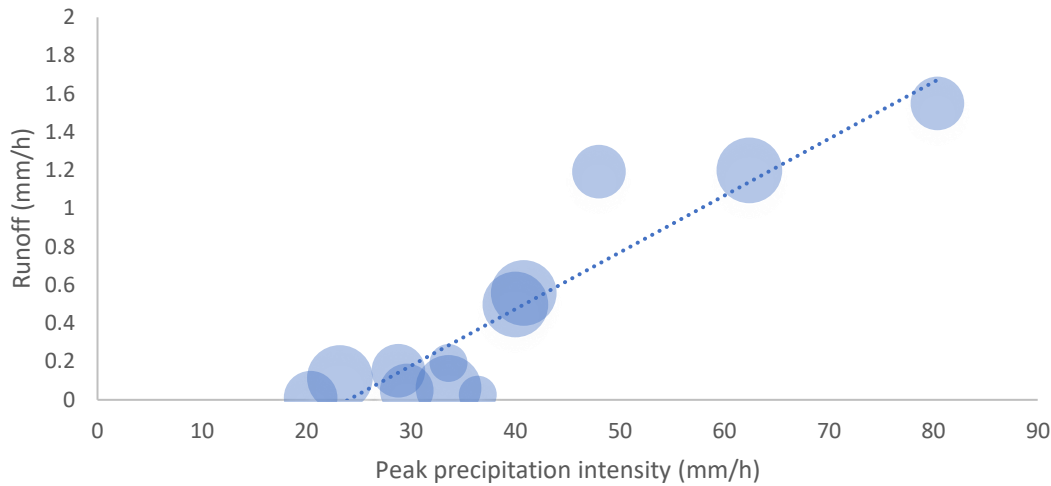
FIGURE 15: SHOWS THE RELATION BETWEEN RUNOFF GENERATION AND PEAK 15 MINUTE PRECIPITATION INTENSITY DURING A RAIN EVENT, THE SIZE OF THE CIRCLES REPRESENT THE CLASS OF SOIL MOISTURE.

The multiple linear regression analysis was conducted on the above researched parameters and the relation between the dependent and independent variables are presented in equation 7.

$$Runoff = -1.09 + 0.0029X_1 + 0.102X_2 + 0.011X_3 + 0.0597X_4 - 0.02X_5 \quad (7)$$

Where -1.09 is the intercept, $X1$ is the event total precipitation amount, $X2$ is the peak 15-minute precipitation, $X3$ is the antecedent soil moisture, $X4$ is the mean hourly precipitation intensity, and $X5$ is the precipitation duration. The constants in front of the independent variables are the regression coefficients which indicate how much a change in the variable effects the dependent variable. The resulting R^2- value from the MLR was 0.996, indicating a strong correlation between the dependent and independent variables. The p-value for the MLR was 5.44 E-7, indicating a significance due to $p<0.05$. The values of significance of the independent variables are presented in table 7.

TABLE 7: MULTIPLE LINEAR REGRESSION ANALYSIS OF RUNOFF GENERATING EVENTS FROM THE HISTORIC TIME SERIES ON SITE 1

Variable	P>|t|
Total Event Precipitation Amount	0.228
Peak 15 min Precipitation	0.000
Antecedent Soil Moisture	0.048
Mean Hourly Precipitation Intensity	0.002
Precipitation Duration	0.063

From the results at the sites, percentiles and median for soil moisture values for the entire soil profile, expressed as volumetric soil water content, and at depth 10, 20, 30, and 40 cm were extracted. The values are listed in tables 8-10.

TABLE 8: SOIL MOISTURE VALUES BEFORE RAIN EVENTS AT SITE 1

Site 1	Volumetric soil moisture content (%)	Soil Moisture 10 cm (%)	Soil Moisture 20 cm (%)	Soil Moisture 30 cm (%)	Soil Moisture 40 cm (%)
5%	23	11	31	33	34
25%	26	16	34	36	36
75%	30	23	37	38	38
95%	33	26	39	40	40
Median	29	24	35	37	37

TABLE 9: SOIL MOISTURE VALUES BEFORE RAIN EVENTS AT SITE 2

Site 2	Volumetric soil moisture content (%)	Soil Moisture 10 cm (%)	Soil Moisture 20 cm (%)	Soil Moisture 30 cm (%)	Soil Moisture 40 cm (%)
5%	16	13	18	18	18
25%	19	17	21	21	21
75%	24	23	26	26	26
95%	27	26	28	28	28
Median	22	21	23	23	23

TABELL 10 : SOIL MOISTURE VALUES BEFORE RAIN EVENTS AT SITE 3

Site 3	Volumetric soil moisture content (%)	Soil Moisture 10 cm (%)	Soil Moisture 20 cm (%)	Soil Moisture 30 cm (%)	Soil Moisture 40 cm (%)
5%	8	7	8	8	8
25%	11	11	11	10	10
75%	15	16	14	14	14
95%	17	18	17	16	16
Median	13	14	13	13	12

To further investigate the effect of the antecedent soil moisture two runoff generating events were extracted from the historic time series. One "dry" event with an antecedent soil moisture of 22 % and one "wet" event with an antecedent wetness of 33 %, the same initial conditions used for the hyetograph simulation. The dry event had an antecedent soil moisture below the field capacity of 28 % while the wet event soil moisture was above the field condition. During

the dry event, the accumulated rainfall accounted to 67 mm, and for the wet event, 37 mm. For both the events, runoff was generated at the same precipitation intensity, at 8,4 mm/h. The runoff, accumulated precipitation, and soil moisture are presented in figures 16 & 17.
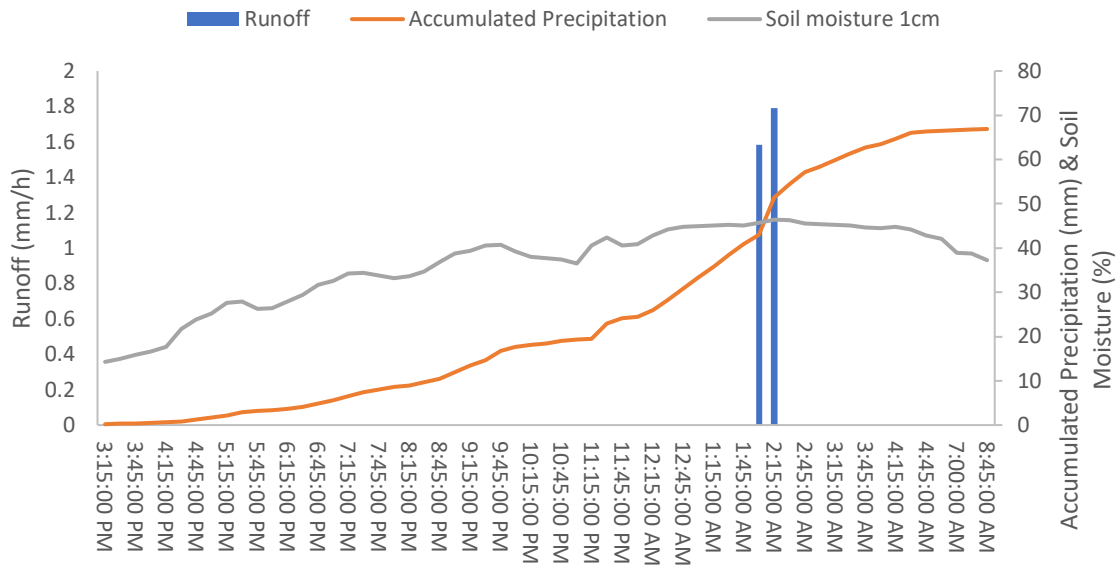
FIGURE 16: HISTORIC RAIN EVENT 24TH JUNE 2010 WITH DRY INITIAL CONDITIONS

The event representing the dry initial condition occurred the 24h June 2010 and started with a soil moisture of 22 % for the entire profile and 14 % at 1 cm depth. For the dry initial condition runoff is first generated after 43 mm accumulated precipitation at a volumetric soil moisture of 55 % and a duration of 12 hours. The rain event lasted for 16 hours, and the peak precipitation was 33,6 mm/h.
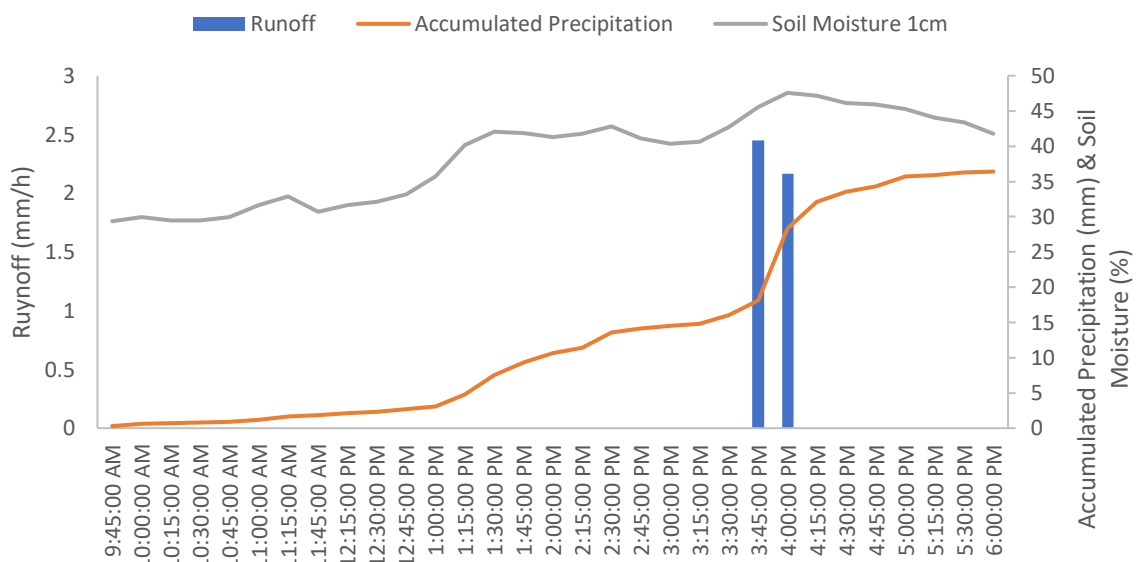
FIGURE 17: HISTORIC RAIN EVENT 29TH JUNE 2010 WITH WET INITIAL CONDITIONS

27

The event representing the wet initial condition occurred five days after the dry event, on the 29th June 2010 and started out with a soil moisture of 33 % for the entire profile and 29 % at 1 cm depth. Runoff was generated after 15 mm accumulated precipitation at a volumetric soil moisture content of 64 % and after a duration of 5 hours. The rain event lasted for 8,25 hours and the peak precipitation was 40,8 mm/h.

5.3 RAIN HYETOGRAPH SIMULATIONS

From the historic rain simulation, the median soil moisture of Site 1 at depths 10, 20, 30, and 40 cm were used as initial conditions for the hyetograph simulations.

Peak precipitation and peak runoff varied greatly for the hyetographs, with hyetograph 4 having the highest values and hyetograph 2 with the lowest values. The total runoff generated by each hyetograph also showed some variation, hyetograph 4 had the highest runoff generation with 31,1 mm whilst hyetograph 2 had the lowest at 23,0 mm. The runoff rate was also highest at hyetograph 4 and the lowest values could be found at hyetograph 2 and 3. Figure 18 depicts the precipitation and runoff generated with the different hyetographs. H4 achieves both the highest runoff generation and precipitation amounts. H1, and partly H2, are the only hyetographs that deviates from an otherwise linear relation between precipitation and runoff.
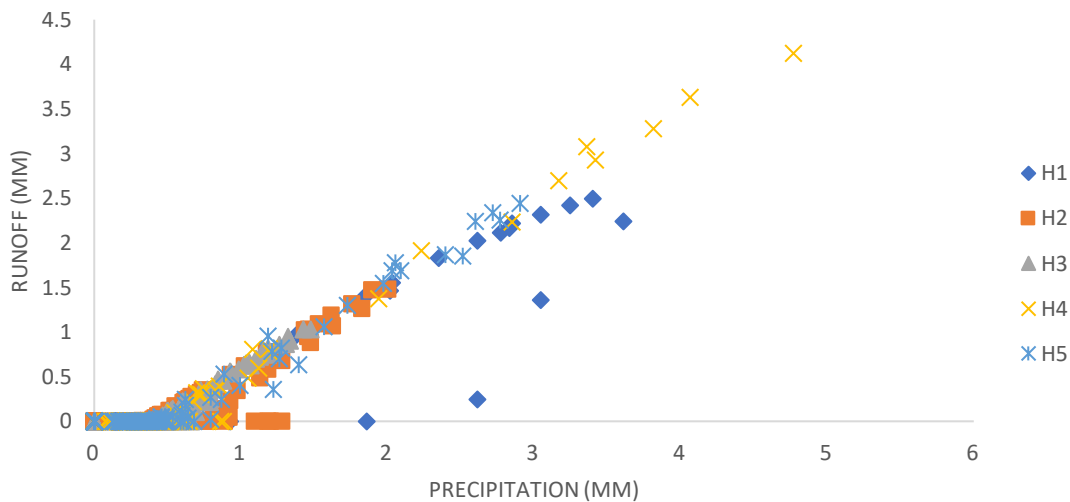
FIGURE 18: GENERATED RUNOFF AND PRECIPITATION AMOUNT AT EACH TIME STEP FOR EACH HYETOGRAPH

Figure 19 shows the results from the simulation of hyetograph 1, characterized by an early peak in precipitation and runoff generation, followed by a low intensity rainfall. Soil moisture increases exponentially at the start of the simulation and continues to increase linearly at 3200 seconds. Runoff generation starts at around 10 mm accumulated rainfall and reaches its peak at 432 seconds. Generally, the runoff generated follows the hyetograph pattern of the peak with the excess water infiltrating into the soil.
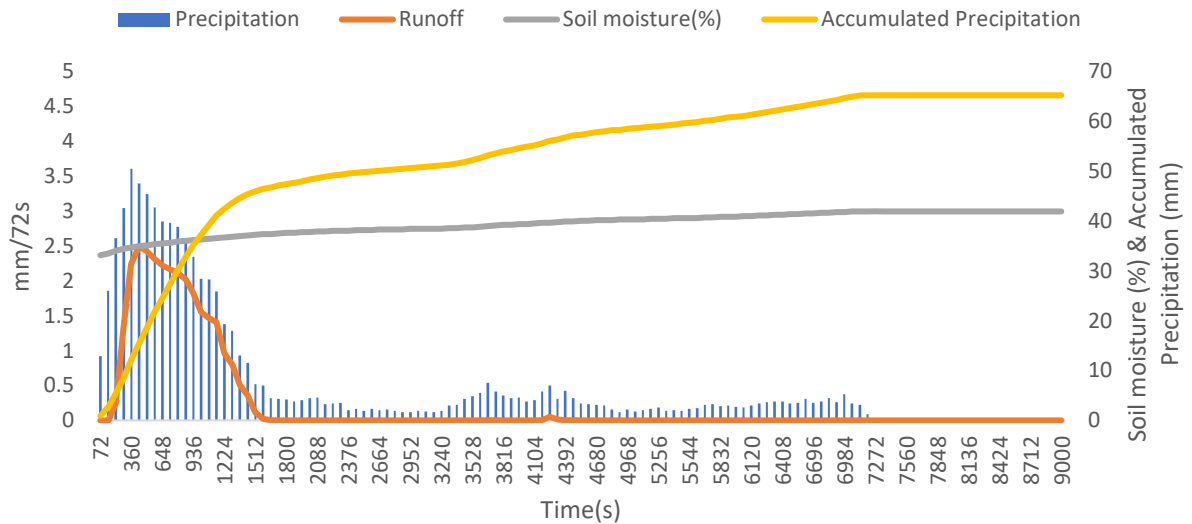
FIGURE 19: HYETOGRAPH 1 ON SITE 1, PRECIPITATION AND RUNOFF PER TIMESTEP PRESENTED ON THE LEFT AXIS, AND SOIL MOISTURE AND ACCUMULATED PRECIPITATION PRESENTED ON THE RIGHT AXIS

The runoff rate from hyetograph 1 presented in figure 20 shows how much of the precipitation generated surface runoff. The main difference from the rainfall-runoff curve seen in figure 19 is how the peak looks in runoff rate, instead of a sharp peak as in figure 19, the peak flats out once reaching rates above 0,75.
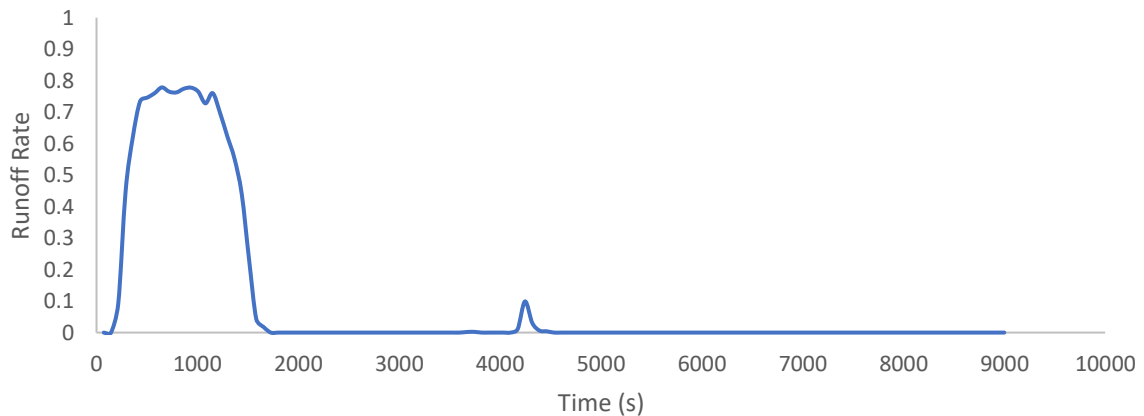
FIGURE 20: RUNOFF RATE DURING THE HYETOGRAPH 1 SIMULATION ON SITE 1.

Figure 21 depicts the simulation of hyetograph 2. This hyetograph is characterized by an early build-up and peak around a quarter into the simulation. Runoff is generated at 10 mm accumulated precipitation and a soil moisture of 35%. The soil moisture increases exponentially at the beginning of the simulation until the peak precipitation is reached, after the peak the soil moisture increases linearly until the rain event is over.
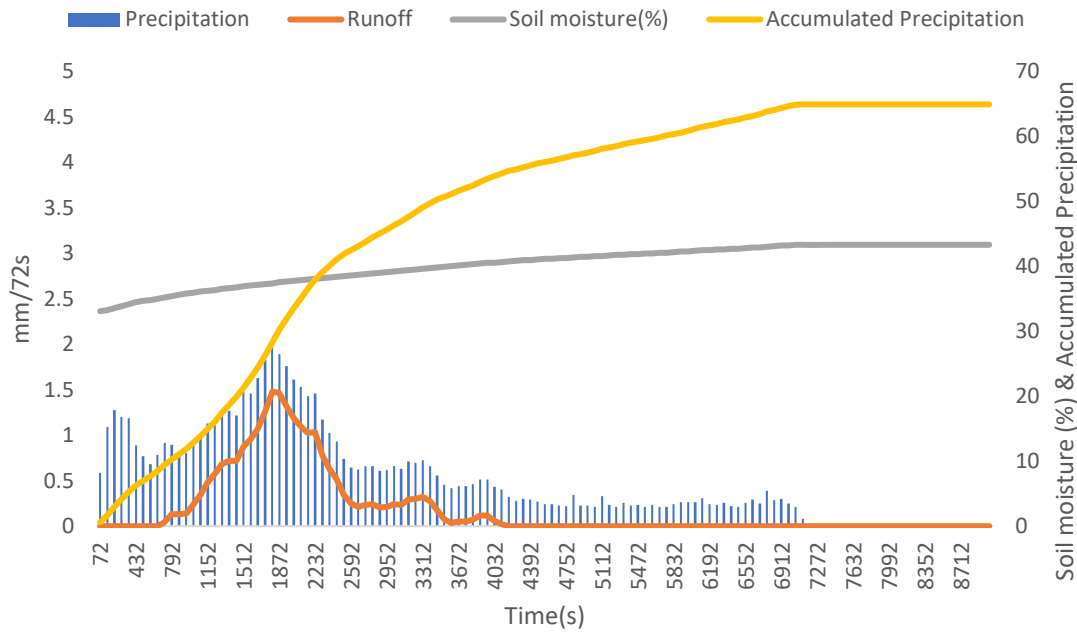
FIGURE 21: HYETOGRAPH 2 SIMULATION ON SITE 1, PRECIPITATION AND RUNOFF PER TIMESTEP PRESENTED ON THE LEFT AXIS, AND SOIL MOISTURE AND ACCUMULATED PRECIPITATION PRESENTED ON THE RIGHT AXIS

In figure 22 the runoff rate starts off by following the hyetograph pattern but after the peak is reached at around 1800 seconds and precipitation is starting to diminish, the decrease in runoff rate is not as prevalent.
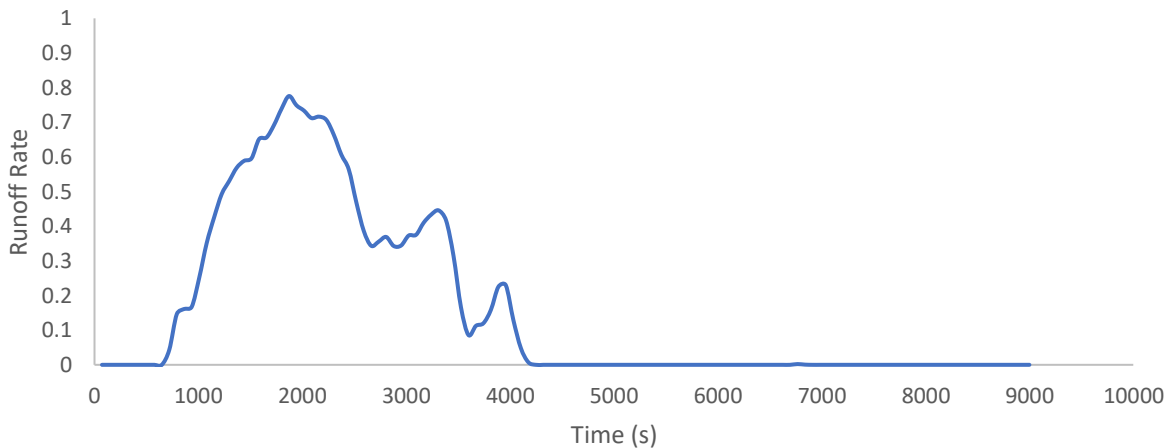
FIGURE 22: RUNOFF RATE DURING THE HYETOGRAPH 2 SIMULATION ON SITE 1.

Figure 23 depicts the rainfall-runoff curve for the hyetograph 3 simulation. This hyetograph is representing a relatively equally temporal distributed rain event with a slight peak at the mid-point. Low amount of runoff is generated at the start of the event but steadily increases as the intensity and soil moisture increase. The soil moisture increases linearly towards the end of the simulation. Runoff is generated at 15 mm accumulated precipitation with a soil moisture of 36%.
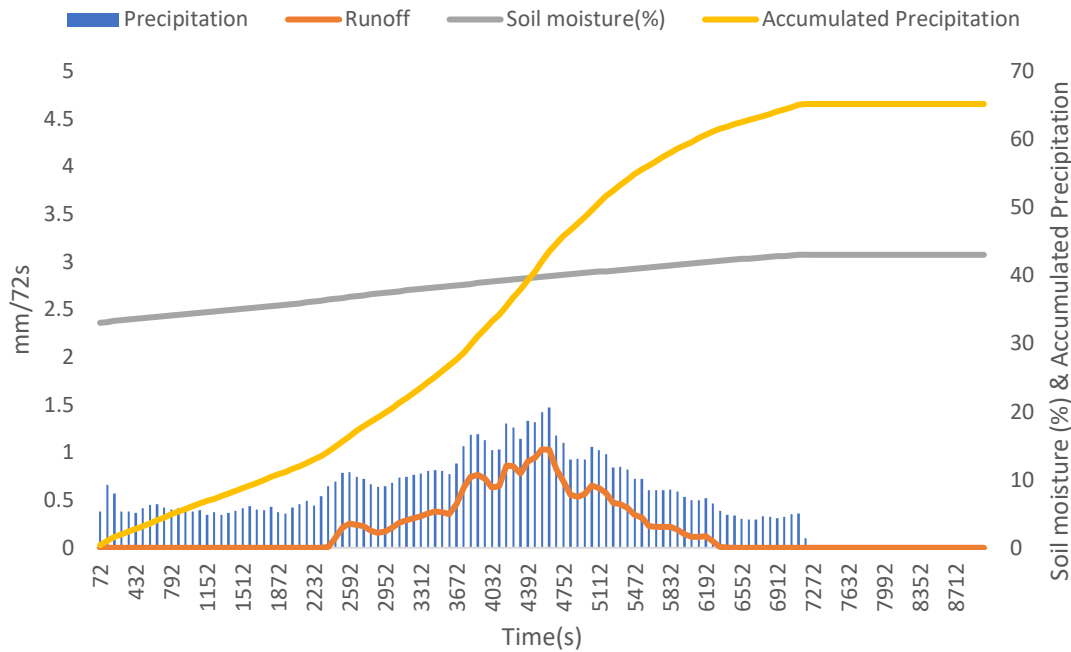
FIGURE 23: HYETOGRAPH 3 ON SITE 1, PRECIPITATION AND RUNOFF PER TIMESTEP PRESENTED ON THE LEFT AXIS, AND SOIL MOISTURE AND ACCUMULATED PRECIPITATION PRESENTED ON THE RIGHT AXIS

Figure 24 shows the runoff rate generated by hyetograph 3 and even though the curve generally follows the same pattern as the hyetograph with a wide peak and equal rate during the build-up and tail-end.
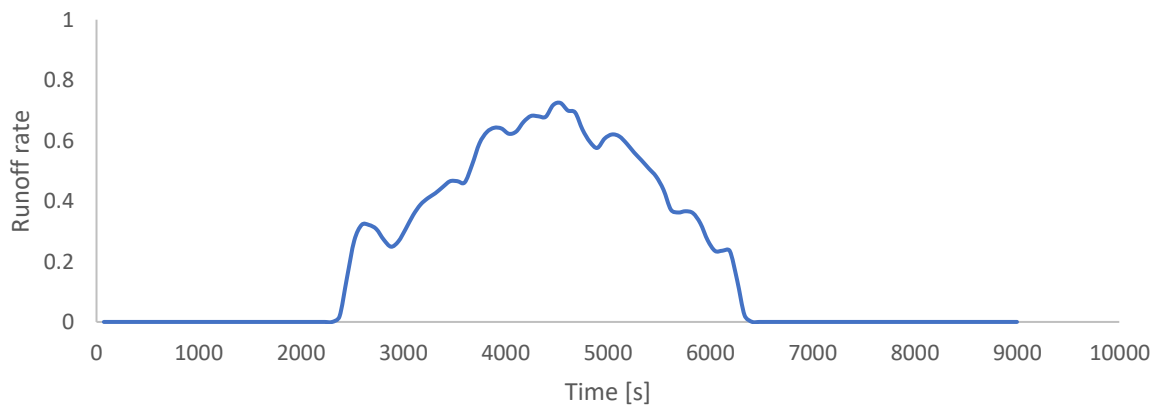
FIGURE 24: RUNOFF RATE DURING THE HYETOGRAPH 3 SIMULATION ON SITE 1.

Figure 25 depicts the precipitation and generated runoff on hyetograph 4. The hyetograph is characterized by irregular rain intensities at the start of the rain event and the highest peak of all the hyetographs in the end of the simulation. The soil moisture increases quite linearly throughout the simulation. Runoff is generated at 23 mm accumulated precipitation and 63% soil moisture.
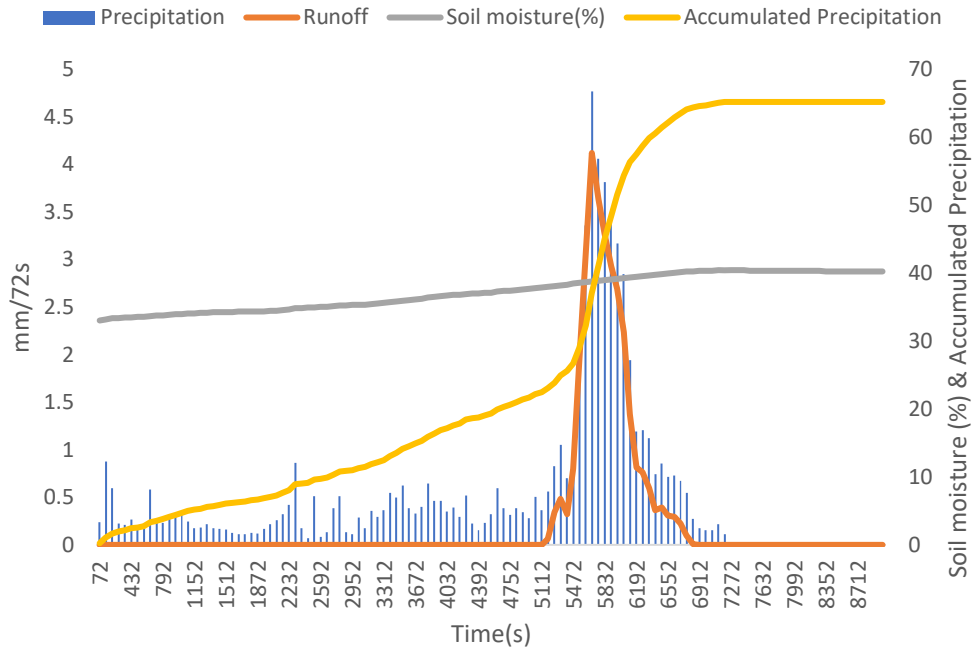
FIGURE 25: HYETOGRAPH 4 ON SITE 1, PRECIPITATION AND RUNOFF PER TIMESTEP PRESENTED ON THE LEFT AXIS, AND SOIL MOISTURE AND ACCUMULATED PRECIPITATION PRESENTED ON THE RIGHT AXIS

Figure 26 shows the runoff rate during the hyetograph 4 simulation. The runoff rates reach a high peak as 90 % of the rainfall is converted to runoff at 5600 seconds, this peak occurs as the highest precipitation intensity of all the hyetographs is simulated, at 239 mm/h.
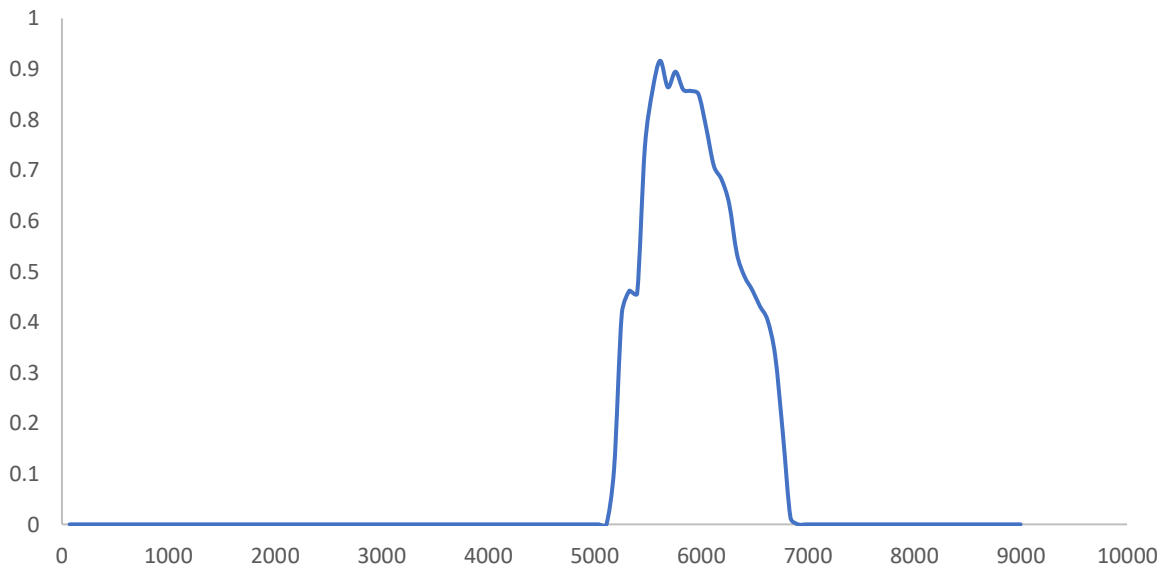
FIGURE 26: RUNOFF RATE DURING THE HYETOGRAPH 4 SIMULATION ON SITE 1.

Figure 27 shows the hyetograph 5 simulation on site 1. This hyetograph is characterized by a low precipitation amount at the start of the simulation with a smaller peak at the middle and the largest peak towards the end. The soil moisture increases quite linearly throughout the event and decreases as the event stops. At the start of the event, all precipitation is infiltrated into the

soil but once the precipitation intensity reaches a value of 40 mm/h runoff is generated. Accumulated rainfall was at 13 mm and soil moisture at 36 % once runoff was generated.
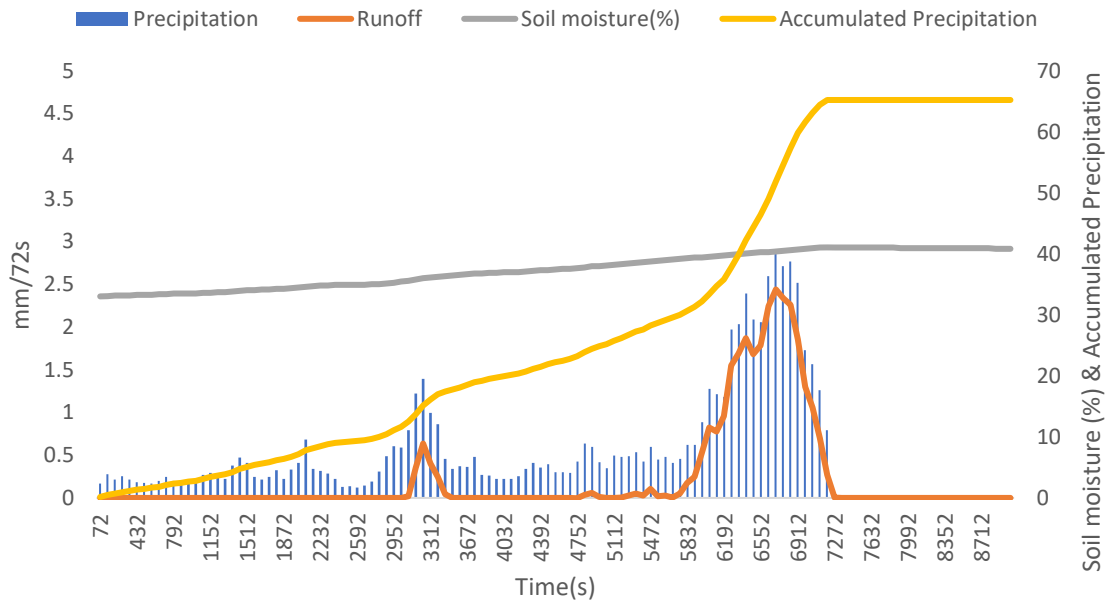
The runoff rate presented in figure 28 is very similar to the pattern seen in figure 27, the two peaks are represented with runoff rates at 0,45 and 0,85. Even though the start of the second peak has a lower precipitation intensity it reaches higher runoff rates than the first peak.
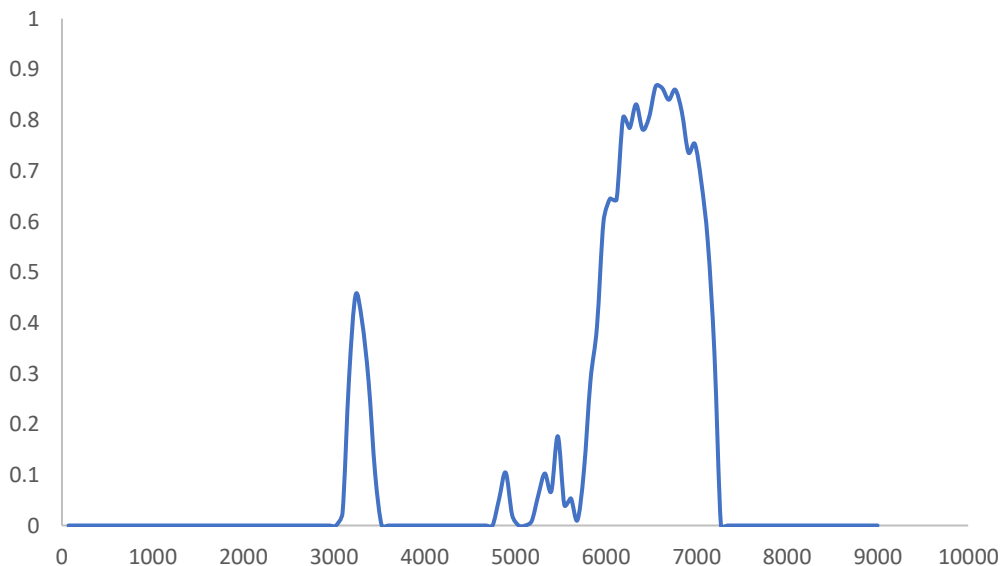
FIGURE 28: RUNOFF RATE DURING THE HYETOGRAPH 5 SIMULATION ON SITE 1.

To summarize the hyetograph simulation, the peak precipitation, peak runoff, total runoff, runoff rate, and the time to the peak from the hyetograph simulations are presented in table 11.

TABLE 11: RESULTS FROM HYETOGRAPH SIMULATION

Hyetograph	Peak Precipitation Intensity (mm/h)	Peak Runoff (mm/h)	Total Runoff (mm)	Runoff Rate (Precipitation/Runoff)	Time to Peak (s)
H1	180	125	29	0,44	360
H2	100	74	23,0	0,35	1800
H3	74	52	24	0,37	3888
H4	239	206	31	0,48	5688
H5	145	117	29	0,44	6696

6. DISCUSSION

6.1 MODEL CONSTRAINTS

The Hydrus 1-D model only simulates the movement of water in one dimension, in this case vertical movement. Therefore, it cannot simulate what Nielsen (2019) considered to be the most dominant rainfall-runoff process from urban pervious areas, subsurface throughflow. Since the bottom boundary condition was set to "Free Drainage" no ground water table was defined which led to saturation excess overland flow only being able to occur if the difference in hydraulic conductivity in the soil was lower than the precipitation intensity. The synthetic area supposed to represent an urban area does not take any vegetation except grass into account. In actuality urban green areas display a much higher diversity of vegetation. Trees are especially important in the rainfall-runoff relation as they have a large leaf area index which is able to intercept a large part of the precipitation. A study by Inkiläinen et.al. (2013) investigated the interception rate during rain events in an urban green area and found out that around 20 % of the precipitation was intercepted by the trees. Had the leaf area index of trees been included in the simulation, lower rates of surface runoff would probably have been seen.

The precipitation data sourced from SMHI measured data every 15 minutes and the lowest measurement recorded was 0.1 mm. Seen in the hyetograph simulations, the temporal variability of a rain event is much greater than 15 minutes. This constraint could lead to missed runoff generation due to precipitation amount being lumped and used to represent the time step. Had the precipitation data been more finely discretised a more precise result had probably been extracted. However, as the retrieved measurements were the best available estimation of precipitation by the time of the study, it was assumed to represent the true precipitation.

The soil moisture values at different depths used as initial conditions for the hyetograph simulations were point values of the respective depths. The value at 10 cm only represents the soil moisture at exact 10 cm depth and the soil moisture values between the point values were interpolated by the Hydrus interface. This should not be considered to be representative of a

real soil due to the often extreme heterogeneity with the presence of macropores, but as it was the only available option it was assumed to be representative of the soils in this study.

6.2 HISTORIC RAIN SIMULATION

The historic rain simulation generated surface runoff from 12 events on site 1, two events on site 2, whilst site 3 did not generate any surface runoff at all. This distribution between the sites can be explained from their respective soil hydraulic properties. Site 1 had the lowest infiltration capacity of the three soils and would therefore be more susceptible to surface runoff as less water is able to infiltrate into the soil. The infiltration capacity for site 2 was about 3 times higher than in site 1, and to get the infiltration capacity for site 3 it had to be multiplied by an additional factor ten.

Out of the 12 rain events that generated runoff on site 1, the two events that generated the most runoff were the only events that could be classed as cloudbursts according to SMHI's definition of at least 1 mm/minute. That only two rain events could be defined as cloudbursts from a 25 – year data series was surprising at first sight but there is an explanation to this. Firstly, due to cloudbursts often occurring locally, the rain gauges used to gather data might have avoided the cloudbursts or only measured them partly. Secondly, the definition used to categorize a rain event required the event to have a duration of at least 2 hours, and due to the often-brief duration of cloudburst, some might be filtered out by the algorithm.

For the 12 events that generated runoff some patterns that would indicate a threshold required for runoff intensities 0,4 mm/h and above at site 1. These thresholds are summarized in table 12.

TABLE 12: THRESHOLD VALUES FOR RUNOFF GENERATION HIGHER THAN 0,4 MM/HR ON SITE 1

Soil Moisture	Rain amount	Rain Duration	Rain Intensity	Peak 15 min Rain intensity
≥28 %	≥20 mm	≤8,5 hours	≥4 mm/hour	≥40 mm/hour

When looking at the main driving forces for runoff generation on the simulated sites, the parameter with the highest degree of linear relation was the peak precipitation intensity during 15 minutes. This would further validate the claim that the main runoff mechanism is infiltration excess overland flow as the largest runoff volumes could be seen at the highest precipitation intensities. This finding was also observed by Jungerius & ten Harkel (1994) when they investigated the influence of rainfall intensity on surface runoff on Dutch coastal dunes. Similar to my findings, they claimed that the total amount of precipitation does not affect the runoff amount noteworthy and that the weekly maximum 30-minute rainfall strongly correlate to the surface runoff generation (Jungerius & ten Harkel, 1994).

Regarding soil moisture at the different sites, they showed great variability before the rain events. The soil at site 1 was the wettest of the three followed by site 2 and lastly site 3. The reason for this was the difference in soil hydraulic properties of the different soils. The upper layers of the sites were all classified as sandy soils, indicating that water easily drains through

this part of the profile. The determining factor for the site's water retention was the lower layers where the fraction of clay at site 1 indicated a higher retention capacity than the other sites. This was also confirmed by the soil moisture values before rain events in tables 8 to 10.

Looking at the accumulated precipitation required for runoff generation, there are some significant differences between the dry and wet event analysis. The dry event pictured in figure 16 required almost three times as much accumulated precipitation before runoff was generated. Additionally, the runoff response from the two events on the same precipitation intensity differ quite a lot as the response from the wet initial conditions is 50 % higher than the dry initial conditions. However, the volumetric soil moisture in the entire profile is 50% higher in the wet initial condition at the time of runoff which would further strengthen the claim that a high antecedent wetness has a positive relation with runoff generation. This was also seen in a soil tank experiment by Song and Wang (2019) where different rain events were simulated on a soil tank while soil moisture and runoff were monitored, and the relation investigated. They found that antecedent soil moisture had a significant impact on runoff generation on their plot scale and found a threshold value for antecedent soil moisture when investigating its relation between the event-based runoff rate. This threshold value was very close the recorded field capacity of the soil (Song & Wang, 2019). These findings are very much in line with the findings from the historic rain series in this study, in which a threshold for runoff generations over 0.4 mm/hour required antecedent soil moisture values of at least 28 %, which also was the field capacity.

The results from the multiple linear regression analysis showed that three of the five investigated parameters had a statistically significant relation with the dependent variable within a 95% confidence interval. These three parameters were peak 15 minute precipitation intensity, mean hourly precipitation intensity, and antecedent soil moisture. The standardized coefficients of the independent variables in equation 7 from the MLR show the overall impact of each variable on the dependent variable, Runoff. From equation 7 the parameter that had the greatest impact on runoff generation was the peak 15-minute precipitation intensity. This further strengthens the claim the peak precipitation intensity is the main driving force for runoff generation on site 1 in this study, but also that the antecedent soil moisture has an impact.

6.3 HYETOGRAPH SIMULATIONS

Out of the five type hyetographs simulated on Site 1, hyetograph 4 was the one that generated the most amount of runoff, totally up to 31.1 mm corresponding to an event-based runoff rate of 0.48. Hyetograph 4 was characterized by a late peak which lasted for 1000 seconds and contained more than 50 % of the total precipitation for the event. Up until the peak there were no runoff generated and instead all the precipitation infiltrated into the soil which caused the soil to reach saturation at the time of the peak. This, together with the highest precipitation intensities of all the hyetographs lead to the highest runoff flows and total runoff generation. The high runoff generation might be mainly due to the high precipitation intensities as the historic time series would insinuate and that soil moisture and temporal distribution might not be a determining factor. To further investigate this, the two hyetographs (1 & 5) that achieved the same total runoff amount but with different peak precipitation intensities was analysed. Hyetograph 1 is characterized by an early peak in which the second highest precipitation

intensity is present followed by low intensity precipitation barely generating any runoff. Hyetograph 5 on the other hand is characterized by a small peak in the middle and a higher peak towards the end of the simulation and a slightly lower peak runoff flow. The peak precipitation was around 25% lower than in hyetograph 1 but the generated runoff was the same for both the hyetographs which would indicate that peak precipitation intensity might not be the sole driving force for high runoff generations. The observed runoff rate for hyetograph 5 reaches higher values than hyetograph 1 and the reason for this could be related to the temporal distribution of the hyetograph.

In general, the reason why runoff rate is increasing in line with the precipitation for the hyetographs is probably due to the runoff being generated by infiltration excess overland flow, when the infiltration capacity of the soil is lower than the precipitation intensity. But comparing the runoff rates from hyetograph 1 and 5 (figure 28 & 20) the runoff rate is much higher at the peak of hyetograph 5 than during the peak of hyetograph 1, even though the rain intensity is lower. This indicates that precipitation intensity is not the only parameter effecting runoff generation. The increased runoff rate could be due to the infiltration capacity of the soil being reached, but since the soil moisture for the profile is steadily increasing during this period and never reaching saturation at 51,27 % this claim cannot be proven. However, the upper parts of the layer might have reached full saturation increasing the runoff rate. To investigate the soil moisture at depth 1 cm was plotted in figure 29 & figure 30.
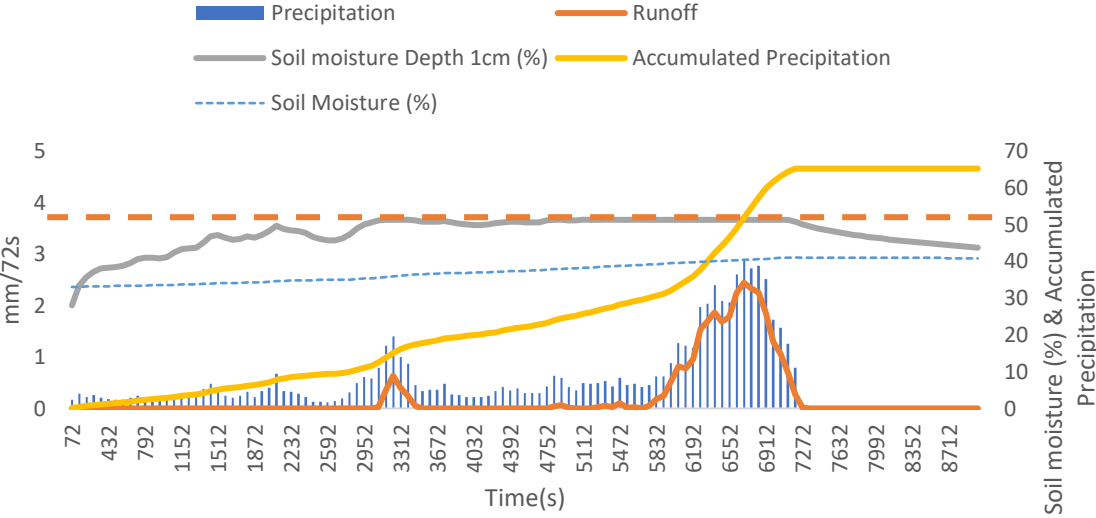
FIGURE 29: SHOWS THE PRECIPITATION, RUNOFF GENERATED AND SOIL MOISTURE AT DEPTH 1 CM, AND ENTIRE PROFILE, SATURATION POINT REPRESENTED BY A DASHED ORANGE LINE FOR HYETOGRAPH 5 SIMULATION ON SITE 1.
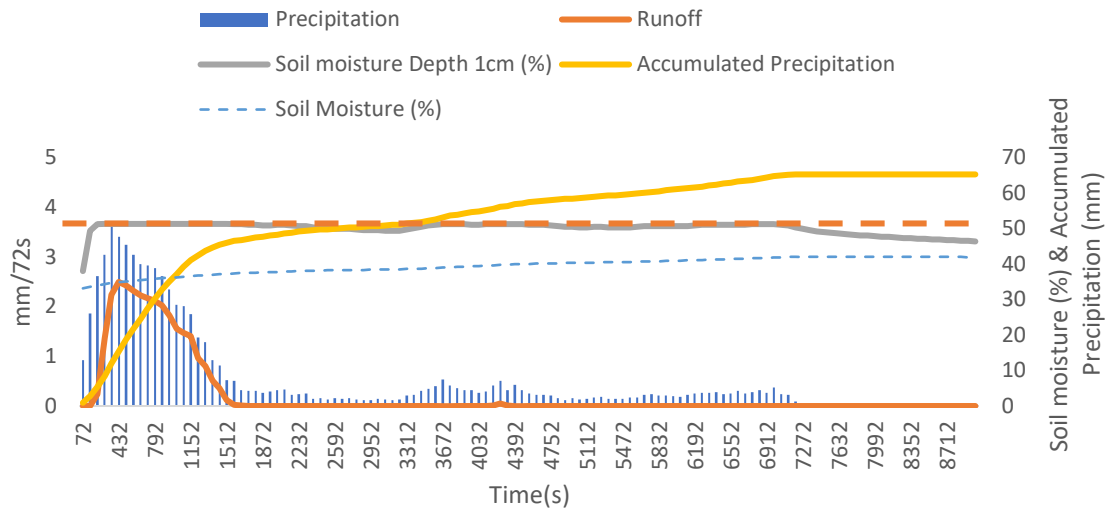
FIGURE 30: THE PRECIPITATION, RUNOFF GENERATED AND SOIL MOISTURE AT DEPTH 1CM, AND ENTIRE PROFILE, SATURATION POINT REPRESENTED BY A DASHED ORANGE LINE FOR HYETOGRAPH 1 SIMULATION ON SITE 1

At depth 1 cm the soil moisture reaches full saturation at the peaks, indicating a completely saturated top layer. The reason why the peak in hyetograph 1 does not reach as high runoff rates as the peak in hyetograph 5 could be that the top layer is not saturated enough in the beginning of the peak to yield such high rates. Most of the precipitation at the start of the peak in hyetograph 1 is infiltrated into the soil before the topmost layer is fully saturated whilst in hyetograph 5, the precipitation peak starts on an already saturated surface, making it less likely to infiltrate. All the surface runoff generated at the peak of hyetograph 5 is a result from both infiltration excess overland flow and saturation excess overland flow (DPSA) while the runoff at the peak of hyetograph 1 is only partly DPSA.

To further investigate this, the infiltration amount during the hyetographs were plotted against the soil moisture in the profile in figure 31. From the figure the lowest infiltration amounts were seen at soil moisture levels above 40 %, close to saturation, whilst the highest infiltration amounts were more common at soil moisture levels close to the field capacity at 28%. The impact of soil moisture on infiltration rate has been investigated in a variety of studies (Cerdà 1996, Castillo et al. 2003, Zehe et al. 2005), and a reoccurring conclusion is that soil is able to infiltrate less water during high soil moisture conditions compared to dryer conditions. Ceballos et al. (2002), conducted a series of sprinkling experiments on a soil in western Spain and studied soil erosion and runoff generation. They found that initial wet conditions resulted in reduced infiltration rates of 50 % in comparison to dry initial conditions. This is very much in line with both the event analysis from the historic time series, but also the hyetograph simulations, mainly H1, H2, and H3. The relation is more obvious for these hyetographs is due to earlier peaks occurring before the top layers are saturated causing high amounts of precipitation to infiltrate rather than run off.
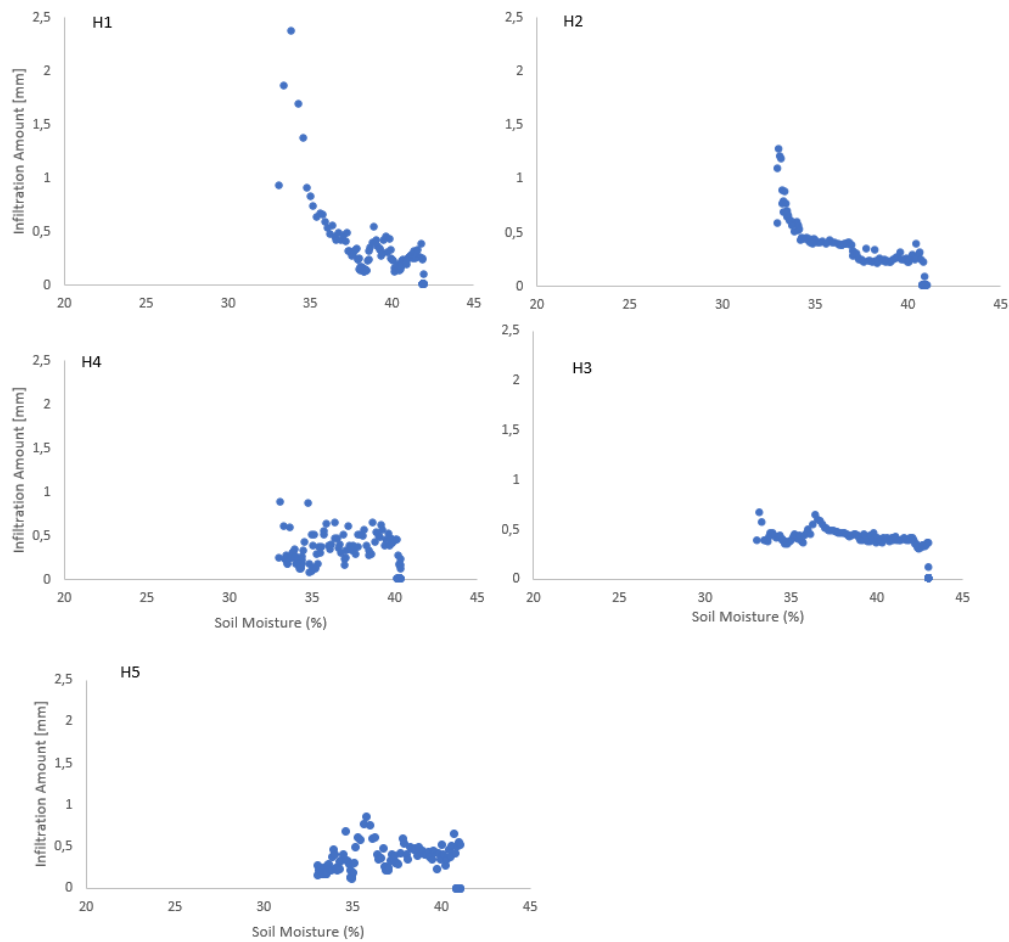
FIGURE 31: SOIL MOISTURE VS INFILTRATION DURING THE HYETOGRAPH SIMULATIONS,

The purpose of the hyetograph simulations was to, with a set precipitation amount and soil hydraulic properties, investigate how the temporal distribution of a heavy rainfall event effect the runoff generated and try to determine the general shape of a rain event capable of generating the most surface runoff. From the simulated hyetographs the highest surface runoff was generated from hyetograph 4, a rain event defined by very high precipitation intensities occurring on a wet soil profile. In general, a soil profile that has been exposed to precipitation to a degree high enough to increase the soil moisture to a point close to saturation will have a reduced capacity to infiltrate further precipitation. If a high intensity rainfall then occurs on this soil surface, high runoff rates is to be expected.

6.4 FUTURE STUDIES

The findings from this study shows that the peak intensity precipitation is the most important out of all the investigated parameters for generating surface runoff on a Swedish green area. The antecedent soil moisture also impacts the surface runoff generation but mainly if it was above field capacity. This study only looks at the surface runoff generation, and from previous studies such as Nielsen (2019) the subsurface throughflow was deemed as the most dominant runoff process in green areas. To get a more complete picture of the runoff generation from green urban areas it would be interesting to scale up the historic series to a park landscape in at least 2 dimensions and find the most important runoff parameters for each of the runoff

generating mechanisms. These parameters could then be represented by a meta parameter which could be used to represent different initial conditions and runoff generations to further ease the modelling process.

It would also be interesting to analyse the impact future climates would have on the runoff generation. As Hydrus is a model that incorporates the Penman-Monteith formula which contains plenty of variables that are directly affected by a changing climate, the resulting runoff generation would probably show some interesting results. These results could then be analysed further and

Another aspect that would be interesting to further study would be the validity of the results presented in this study. My study showed the Hydrus simulated runoff generation on three different soils, and the validity of the results were confirmed by comparing them to the findings of earlier studies. It would be interesting to compare the results with other commonly used rainfall-runoff models and try to work out the differences. The hyetograph simulation or a block rain simulation could be used to also be able emulate them in a laboratory environment which could act as an answer template.

7. CONCLUSIONS

- **How does antecedent soil moisture impact the generation of surface runoff from a Swedish green urban area?**

The antecedent soil moisture had a significant relation to runoff generation within a 95 % confidence interval. From the historic time series surface runoff were only generated is the soil moisture level was at least at field capacity at site 1. When comparing generated surface runoff on a soil with dry and wet initial conditions, the wet initial conditions generated surface runoff at a rate 50% higher than the dry conditions. The wet conditions also needed less than 50 % the precipitation amount to generate runoff. From the type hyetograph simulations the conclusion that a high antecedent soil moisture would generate higher amount of surface runoff than low antecedent soil moisture in this study could be drawn.

- **What is the main driving force for surface runoff generation on a Swedish green urban area?**

From the graphical analysis together with the multiple linear regression analysis the main driving force for surface runoff generation on the investigated Swedish green urban area was peak 15-minute precipitation intensity. The threshold value for site 1 was that a rain event should include a peak 15-minute precipitation intensity of at least 40 mm/h to generate surface runoff. Other noteworthy parameters that effect runoff generation was antecedent soil moisture and mean precipitation intensity.

- **What soil moisture content was present in the soil before rain events in Sweden?**

The soil moisture content in the soil before rain events in Sweden were gathered from an historic precipitation series from two weather stations in Stockholm spanning from 1997-01-01 to 2022-01-01. An algorithm separated the rain events into singular events and the

soil moisture value at the first timestep of the event was used for the antecedent soil moisture. Out of the three sites, Site 1 had a median volumetric antecedent soil moisture of 29 %, Site 2 had 22%, and site 3 had 13 %.

- **Does the temporal distribution of a rain event effect runoff generation?**

The temporal distribution of a rain event does influence runoff generation, proven by the hyetograph simulations, a rain event in which low intensity rainfall is allowed to infiltrate into the soil profile followed by a high intensity peak will result in high runoff generation. In contrast, an early peak in precipitation intensity followed by low intensity rainfall, and a wide peak in precipitation will results in lower runoff generation.

References

Allen, R. G., Pereira, L. S., Raes, D., & Smith, M. (1998). Crop evapotranspiration-guidelines for computing crop water requirements (p. 56). FAO.

Anees, M. T., Abdullah, K., Nawawi, M. N. M., Ab Rahman, N. N. N., Piah, A. R. M., Zakaria, N. A., Syakir, M. I., & Mohd. Omar, A. K. (2016). Numerical modeling techniques for flood analysis. *Journal of African Earth Sciences*, *124*, 478–486. https://doi.org/10.1016/J.JAFREARSCI.2016.10.001

Berti, A., Tardivo, G., Chiaudani, A., Rech, F., & Borin, M. (2014). Assessing reference evapotranspiration by the Hargreaves method in north-eastern Italy. *Agricultural Water Management*, *140*, 20–25. https://doi.org/10.1016/j.agwat.2014.03.015

Beven, K. (2012). Rainfall-Runoff Modelling: The Primer: Second Edition. *Rainfall-Runoff Modelling: The Primer: Second Edition*, 1–457. https://doi.org/10.1002/9781119951001

Birkel, C., & Barahona, A. C. (2019). Rainfall-Runoff Modeling: A Brief Overview. *Reference Module in Earth Systems and Environmental Sciences*. https://doi.org/10.1016/B978-0-12-409548-9.11595-7

Broekhuizen, I., Muthanna, T. M., Leonhardt, G., & Viklander, M. (2019). Urban drainage models for green areas: Structural differences and their effects on simulated runoff. *Journal of Hydrology X*, *5*. https://doi.org/10.1016/J.HYDROA.2019.100044

Broekhuizen, I., Sandoval, S., Gao, H., Mendez-Rios, F., Leonhardt, G., Bertrand-Krajewski, J. L., & Viklander, M. (2021). Performance comparison of green roof hydrological models for full-scale field sites. *Journal of Hydrology X*, *12*, 100093. https://doi.org/10.1016/J.HYDROA.2021.100093

Buda, A. R. (2013). Surface-Runoff Generation and Forms of Overland Flow. *Treatise on Geomorphology*, *7*, 73–84. https://doi.org/10.1016/B978-0-12-374739-6.00151-2

Caiqiong, Y., & Jun, F. (2016). Application of HYDRUS-1D model to provide antecedent soil water contents for analysis of runoff and soil erosion from a slope on the Loess Plateau. *Catena*, *139*, 1–8. https://doi.org/10.1016/j.catena.2015.11.017

Certified Crop Advisor study resources (Northeast region). (n.d.). Retrieved November 4, 2022, from https://nrcca.cals.cornell.edu/soil/CA2/CA0211.1.php

Chaudhari, P. R., Ahire, D. V, Ahire, V. D., Chkravarty, M., & Maity, S. (2013). Soil Bulk Density as related to Soil Texture, Organic Matter Content and available total Nutrients of Coimbatore Soil. *International Journal of Scientific and Research Publications*, *3*(2). www.ijsrp.org

European Union. (2013). *Hard surfaces, hidden costs Searching for alternatives to land take and soil sealing Environment*. https://doi.org/10.2779/16427

Gregory, J. H., Dukes, M. D., Miller, G. L., & Jones, P. H. (2005). Analysis of Double-Ring Infiltration Techniques and Development of a Simple Automatic Water Delivery System. *Applied Turfgrass Science*, *2*(1), 1–7. https://doi.org/10.1094/ATS-2005-0531-01-MG

Islam, Z. (2011). *A Review on Physically Based Hydrologic Modeling*. https://www.researchgate.net/publication/272169378_A_Review_on_Physically_Based_Hydrologic_Modeling

Johnson, A. I. (1963). A Field Method for Measurement of Infiltration. *Soil Science Society of America Journal*, *20*(3), 430–440.

https://doi.org/10.2136/sssaj1956.03615995002000030036x

Jungerius, P. D., & ten Harkel, M. J. (1994). The effect of rainfall intensity on surface runoff and sediment yield in the grey dunes along the Dutch coast under conditions of limited rainfall acceptance. *Catena*, *23*(3–4), 269–279. https://doi.org/10.1016/0341-8162(94)90072-8

Kiani-Harchegani, M., Talebi, A., Asgari, E., & Rodrigo-Comino, J. (2022). Topographical features and soil erosion processes. *Computers in Earth and Environmental Sciences*, 117–126. https://doi.org/10.1016/B978-0-323-89861-4.00034-8

Knutsson, G., & Morfeld, C.-O. (1973). *Vatten i jord och berg*. Ingenjörsförlaget.

MSB. (2017). *Vägledning för skyfallskartering : tips för genomförande och exempel på användning*.

MSB (Swedish Civil Contingencies Agency). (2012). *Översvämningar i Sverige 1901–2010*.

Nielsen, K. . (2019). Monitoring of Rainfall-Runoff from Urban Pervious Areas. In G. Balint, B. Antala, C. Carty, J.-M. A. Mabieme, I. B. Amar, & A. Kaplanova (Eds.), *Uniwersytet śląski* (Vol. 7, Issue 1). Aalborg Universitetsforlag. https://doi.org/10.2/JQUERY.MIN.JS

Olsson, J., Berg, P., Eronn, A., Simonsson, L., Södling, J., Wern, L., & Yang, W. (2017). Extremregn i nuvarande och framtida klimat Analyser av observationer och framtidsscenarier. In *KLIMATOLOGI* (Vol. 47).

Olsson, J., Berg, P., Eronn, A., Simonsson, L., Wern, L., & Yang, W. (2017). *Extremregn i nuvarande och framtida klimat*. *47*.

Oosterbaan, R., & Nijland, H. (1986). Determining the Saturated Hydraulic Conductivity. *Drainage Principles and Applications*, 37. https://www.researchgate.net/publication/265217207_Determining_the_saturated_hydraulic_conductivity

Rai, R. K., Singh, V. P., & Upadhyay, A. (2017). Soil Analysis. *Planning and Evaluation of Irrigation Projects*, 505–523. https://doi.org/10.1016/B978-0-12-811748-4.00017-0

Ravn, H., Davidsen, S., Löwe, R., Ravn, N. H., Jensen, L. N., & Arnbjerg-Nielsen, K. (2018). General rights Initial conditions of urban permeable surfaces in rainfall-runoff models using Horton's infiltration Initial Conditions of Urban Permeable Surfaces in Rainfall-Runoff Models Using Horton's Infiltration. *Water Science and Technology*, *77*(3), 662–668. https://doi.org/10.2166/wst.2017.580

Reimann, R. (n.d.). *Synthetic Data*.

SCB. (2015). *Grönytor och grönområden i tätorter 2015*. www.scb.se

Shi, W., Wang, M., Li, D., Li, X., & Sun, M. (2022). An improved method that incorporates the estimated runoff for peak discharge prediction on the Chinese Loess Plateau. *International Soil and Water Conservation Research*. https://doi.org/10.1016/J.ISWCR.2022.09.001

Šimunek, J., Genuchten, M. T. van, & Šejna, M. (2012). HYDRUS: Model Use, Calibration, and Validation. *Transactions of the ASABE*, *55*(4), 1263–1274. https://doi.org/10.13031/2013.42239

Song, S., & Wang, W. (2019). Impacts of Antecedent Soil Moisture on the Rainfall-Runoff Transformation Process Based on High-Resolution Observations in Soil Tank Experiments. *Water 2019, Vol. 11, Page 296*, *11*(2), 296. https://doi.org/10.3390/W11020296

Starzec, M., Dziopak, J., & Słyś, D. (2020). *An Analysis of Stormwater Management Variants in Urban Catchments*.

Steenhuis, T. S., Agnew, L., Gérard-Marchant, P., & Walter, M. T. (2005). OVERLAND FLOW. *Encyclopedia of Soils in the Environment*, *4*, 130–133. https://doi.org/10.1016/B0-12-348530-4/00568-3

Svenskt Vatten. (2007). *Klimatförändringarnas inverkan på allmänna avloppssystem Underlagsrapport till Klimat-och sårbarhetsutredningen*.

Svenskt Vatten AB. (2016). *P110 Avledning av dag-,drän- och spillvatten*.

Sveriges Geologiska Undersökning. (n.d.). *Jordarter 1:25000-1.100000*.

van Genuchten, M. T., Schaap, M. G., & Leij, F. J. (2001). Rosetta: a computer program for estimating soil hydraulic parameters with hierarchial pedotransfer functions. *Journal of Hydrology X*, *251*(3–4), 163–176. https://doi.org/10.1016/S0022-1694(01)00466-8.

Wang, Y., Gao, L., Huang, S., & Peng, X. (2022). Combined effects of rainfall types and antecedent soil moisture on runoff generation at a hillslope of red soil region. *European Journal of Soil Science*, *73*(4). https://doi.org/10.1111/ejss.13274

Weiler, M., Mcdonnell, J. J., Meerveld, I. T., & F, E. P. (2006). *112 : Subsurface Stormflow*. 1–14.

Yasuda.H, Katsura, M. Katsuragi, H. (2023) Grain-size dependence of water retention in a model aggregated soil, Advanced Powder Technology, 34, doi:10.1016/j.apt.2022.103896.

Zehe, E., *et al.*, 2005. Uncertainty of simulated catchment runoff response in the presence of threshold processes: Role of initial soil moisture and precipitation. *Journal of Hydrology*, 315 (1–4), 183–202. doi:10.1016/j.jhydrol.2005.03.038

Appendix

Appendix A1: Soil Properties

TABLE A1 1: SOIL PROPERTIES FROM FIELD EXPERIMENT

MEDEL ÖVRE LAGER	Site 1	Site 2	Site 3	SOIL TEXTURE TRIANGL
1	2,63470369	79,3067513	18,058545	LOAMY SAND
2	3,63022372	75,9075559	20,4622203	LOAMY SAND
3	2,00083805	89,2447224	8,75443951	SAND
MEDEL UNDRE LAGE	Site 1	Site 2	Site 3	SOIL TEXTURE TRIANGL
1	36,4393294	47,9710145	15,5896562	SANDY CLAY
2	4,95169082	63,1642512	31,884058	SANDY LOAM
3	0,86580087	90,2958153	8,83838384	SAND

TABLE A1 2: SOIL PROPERTIES FROM FIELD EXPERIMENT

Prov	Lera	Sand	Silt	Total Höjd	% LER	% SAND	%SILT
GÖP1	3	57	20	80	3,75	71,25	25
GUP1	35	45	12	92	38,04347826	48,9130435	13,0434783
GÖP2	2	75	15	92	2,173913043	81,5217391	16,3043478
GUP2	35	45	20	100	35	45	20
GÖP3	2	86	13	101	1,98019802	85,1485149	12,8712871
GUP3	37	51	14	102	36,2745098	50	13,7254902
BÖP1	3	78	22	103	2,912621359	75,7281553	21,3592233
BUP1	4	60	28	92	4,347826087	65,2173913	30,4347826
BÖP2	4	70	18	92	4,347826087	76,0869565	19,5652174
BUP2	5	55	30	90	5,555555556	61,1111111	33,3333333
ÅÖP1	1	65	8	74	1,351351351	87,8378378	10,8108108
ÅUP1	0	55	5	60	0	91,6666667	8,33333333
ÅÖP2	4	77	5	86	4,651162791	89,5348837	5,81395349
ÅUP2	2	68	7	77	2,597402597	88,3116883	9,09090909
ÅÖP3	0	75	8	83	0	90,3614458	9,63855422
ÅUP3	0	70	7	77	0	90,9090909	9,09090909

TABLE A1 3: SOIL PROPERTIES FROM FIELD EXPERIMENT

Prov	Weight total(g)	Weight container(g)	Weight soil(g)	Bulk density g/cm	AVERAGE BD UPPER	
GÖP1	383,53	133,6	249,93	1,243049841	GEO	1,2752953
GUP1	403,03	145,7	257,33	1,279854422	BMC	1,28494133
GÖP2	406,63	146,57	260,06	1,293432328	ÅNGAN	1,33968673
GUP2	403,16	151,57	251,59	1,251306004		
GÖP3	403,91	144,66	259,25	1,289403719	AVERAGE BD LOWER	
GUP3	402,03	149,7	252,33	1,254986462	GEO	1,26204896
BÖP1	419,92	155,6	264,32	1,31461983	BMC	1,28995081
BUP1	410,73	155,5	255,23	1,269409879	ÅNGAN	1,32220456
BÖP2	380,49	147,1	233,39	1,255262833		
BUP2	409,29	145,8	263,49	1,310491749		
ÅÖP1	402,31	147,7	254,61	1,266326252		
ÅÖP2	425,38	147,1	278,28	1,384051174		
ÅUP2	412,03	144	268,03	1,333071856		
ÅÖP3	426,49	151,3	275,19	1,368682775		
ÅUP3	405,86	142,2	263,66	1,311337259		

Appendix A2: Python programming

CODE A2 1: RAIN EVENT ALGORITHM

```python
import datetime as dt
import numpy as np
import pandas as pd
Precipitation =
pd.read_csv(r'C:\Tyrens\HYDRUS\PythonVärden\Precipitation.txt',
                sep ='\t',
                index_col=0,
                parse_dates=True,
                decimal = ',')
Precipitation = Precipitation.loc[~(Precipitation==0).all(axis=1)]

ts = (Precipitation.index.values[1:] - Precipitation.index.values[:-1])  /
pd.Timedelta('1min')
ts = np.concatenate([[np.nan], ts])
Precipitation['ts'] = ts
Precipitation['mm_min'] = Precipitation['Precipitation']/ts

Precipitation['new_event'] = 0
Precipitation.loc[Precipitation['ts']>180, 'new_event']= 1
Precipitation['event'] = Precipitation['new_event'].cumsum()
events = Precipitation.reset_index().groupby('event').agg(
    {
    'Precipitation': sum,
    'Datum': ('first', 'last',)

    }
    )
events.columns = ['Precipitation', 'start', 'end']

events['duration_hr'] = (events['end']- events['start']) /
pd.Timedelta('1hr')
events['intensity_mmrhr'] = events['Precipitation']/events['duration_hr']
```

```python
nyregn = events.query('duration_hr>2 and Precipitation >=2')

Tid = nyregn[['start', 'end']]
```

CODE A2 2: RUNOFF GENERATION, PERCENTILES, SOIL MOISTURE

```python
import pandas as pd
import numpy as np
import datetime as dt
from statistics import mean

Lera = pd.read_csv(r'C:\Tyrens\HYDRUS\Lera.csv',
                   sep =',',
                   index_col = 0,
                   parse_dates = True
                   ) #Importerar matris med regn, markmättnad, avrinning,
tid
Lera = Lera[Lera['Precipitation'] !=0] # Sorterar ut värden då nederbörd =
0
ts = (Lera.index.values[1:]-Lera.index.values[:-1]) / pd.Timedelta('1min')
ts = np.concatenate([[np.nan],ts])
Lera['ts'] = ts
Lera['mm_min'] = Lera['Precipitation']/ts #Tar fram minutvärden från 15 min
intervallen

Lera['new event']  = 0
Lera.loc[Lera['ts']>180, 'new event']=1   # definierar ett event som en
tidsperiod över 180 min = 3h
Lera['event'] = Lera['new event'].cumsum()
events = Lera.reset_index().groupby('event').agg(
    {
    'Precipitation': (sum, max),
    'RunOff': (sum, max),
    'sum(RunOff)': ('first', 'last'),
    'Volume': ('first', 'last'),
    'theta1': ('first', 'last'),
    'theta10': ('first', 'last'),
    'theta20': ('first','last'),
    'theta30': ('first','last'),
    'theta40': ('first','last'),
    'Datum': ('first', 'last')
    }
    )
events.columns = ['Precipitationsum','Percipmax','RunOffsum','Runoffmax',
'SumRe', 'SumRs','Volumes','Volumee','theta1s','theta1e',
'theta10s','theta10e', 'theta20s','theta20e', 'theta30s','theta30e',
'theta40s','theta40e', 'start', 'end']

events['duration_hr'] = (events['end'] - events['start']) /
pd.Timedelta('1hr')
events['intesity_mmhr'] = events['Precipitationsum']/events['duration_hr']

LRegn = events.query('duration_hr>2 and Precipitationsum >= 2')

LeraProc = LRegn[['Volumes','theta1s','theta10s','theta20s', 'theta30s',
'theta40s']].quantile([0.05, 0.25, 0.75, 0.95]) #Tar ut 25, 75, 95
precentilen
LeraMedian = LRegn[['Volumes','theta1s', 'theta10s', 'theta20s',
'theta30s', 'theta40s']].median()
```

CODE A2 3: MULTIPLE LINEAR REGRESSION ANALYSIS

```
import pandas as pd
from sklearn import linear_model
import statsmodels.api as sm

Multi = pd.read_excel('/Applications/EXJOBB/Multi.xlsx') #Resultatfil

#Multi.drop(Multi.tail(1).index,inplace=True) #Tar bort sista raden i min data pga innehöll ej värden
(OBS:Specifikt för min indatafil)

data = {'Precipitation': Multi['Precipitation'],
    'ASM': Multi['ASM'],
    'Peak_Precipitation': Multi['Percipmax'],
    'Duration': Multi['duration_hr'],
    'intensity_mmhr': Multi['intesity_mmhr'],
    'Runoff': Multi['RunOff(mm/h)']
}
df = pd.DataFrame(data)

x = df[['Peak_Precipitation','ASM', 'intensity_mmhr', 'Precipitation', 'Duration']] #Independent variables som
används för att hitta ett samband till avrinning
y = df['Runoff'] #Dependent variable, i detta fall avrinning


#Statsmodels
x = sm.add_constant(x) # adding a constant

model = sm.OLS(y, x).fit() # Ordinary least square metoden
predictions = model.predict(x)

print_model = model.summary()
print(print_model)
```